

RESEARCH TECHNICAL REPORT

*Large-Scale Testing of Oxygen
Reduction Systems for ASRS
and Frozen Food Applications*



***Large-Scale Testing of Oxygen Reduction Systems for ASRS and
Frozen Food Applications***

Prepared by

Stanislav Kostka

Prepared for

Property Insurance Research Group

October 2024

FM

1 Technology Way
Norwood, MA 02062

PROJECT ID RW000215

Disclaimer

The research presented in this report, including any findings and conclusions, is for informational purposes only. Any references to specific products, manufacturers, or contractors do not constitute a recommendation, evaluation or endorsement by Factory Mutual Insurance Company (FM) of such products, manufacturers or contractors. FM does not address life, safety, or health issues. The recipient of this report must make the decision whether to take any action. FM undertakes no duty to any party by providing this report or performing the activities on which it is based. FM makes no warranty, express or implied, with respect to any product or process referenced in this report. FM assumes no liability by or through the use of any information in this report.

Executive Summary

An oxygen reduction system (ORS) provides fire protection by creating a low oxygen environment in a protected space. In certain applications, ORS can be used as an alternative means of protection instead of traditional sprinklers. Whereas sprinkler protection uses water spray to cool fuel surfaces and suppress fire growth, ORS are designed to reduce the ambient oxygen level low enough that fire cannot propagate. The key design parameter that guides an ORS's ability to prevent fire growth is the limiting oxygen concentration for fire propagation (LOC_{FP}). The LOC_{FP} defines the concentration of oxygen necessary for protection and depends on various factors including the ignition source, test method, and the stored commodity. It becomes important to know this value, as lowering oxygen concentration in a space typically results in occupancy restrictions, additional safety requirements set by occupational health and safety regulations, and increased cost to generate and maintain lower oxygen concentrations.

Small and large-scale testing approaches have been used in the past to evaluate the LOC_{FP} for various commodities. Large-scale testing is preferred since it provides the ability to evaluate representative storage geometries and material compositions present in actual warehouse applications. Previous work has been performed on FM standard commodities. The current work used a large-scale test enclosure to determine the LOC_{FP} of mini-load automatic storage and retrieval systems (ML-ASRS) and high-moisture-content frozen food storage. Given the differences in storage geometry for ASRS arrangements and the lower temperatures and higher moisture contents found in frozen food applications, those storage configurations were evaluated in this work to understand any requisite changes to the LOC_{FP} that may result from the altered conditions. These two applications are of particular interest because the limited personnel present in ASRS and the challenges of using water-based protection in freezers represent conditions that are well aligned with the advantages of ORS fire protection.

In ML-ASRS configurations, the mass of the containers contributed to differences in LOC_{FP} , ultimately yielding an LOC_{FP} of 14.5% oxygen for empty containers or those filled with non-combustible contents. The contents of the containers were also found to be important and changed the LOC_{FP} . Contents stored in corrugated boxes (*e.g.*, cartoned commodities) resulted in LOC_{FP} values consistent with that of standard cartoned commodities at 11% oxygen. Exposed plastic contents brought the LOC_{FP} to 13%. A wider flue space resulted in higher LOC_{FP} , possibly driven by decreased participation of combustible materials around the ignition zone. It is expected that alternative ignition scenarios could increase material available for combustion leading to LOC_{FP} matching the values measured for narrow flue space.

Frozen food, consisting of frozen meals packaged in corrugated cardboard, behaved similarly to FM standard cartoned commodities in reduced oxygen. Fire growth was driven by the external packaging material. However, the inclusion of the frozen contents provided a slight protection benefit, indicated by a marginally higher LOC_{FP} of 12.5% for the frozen food as opposed to 11% for standard cartoned commodities. The benefit was attributed to the low temperature and large thermal inertia of the frozen food, which resulted in minimal fire damage to the commodity and minimal lateral fire spread in the array.

As highlighted in this and previous works, the LOC_{FP} has been shown to depend on storage material, geometry, and test conditions. It is important to note that the recommendations provided in this report are based on the conditions tested. Although engineering judgment can be used to further expand on the current recommendations, factors such as ignition scenario or stored material characteristics may result in changes to the LOC_{FP} that would require additional testing to determine. Efforts to improve the ability of small-scale testing to match results from large-scale experiments are important and will help improve future efforts involving different commodities.

Abstract

This work evaluated the use of oxygen reduction systems (ORS) for fire protection of automatic storage and retrieval systems (ASRS) and high-moisture-content frozen food storage applications. A large-scale test enclosure with a variable ambient oxygen concentration was used to determine the limiting oxygen concentration for fire propagation (LOC_{FP}) for each application. Each test configuration was ignited with a premixed burner, providing a stable exposure for a period of ten minutes. Test outcome was defined by the level of fire propagation in the fuel array over the ignition duration. The tested oxygen concentration was deemed to provide acceptable protection if the fire did not grow beyond the test array during the ignition duration. Results show that the container geometry and quantity of participating material have noticeable effects on the LOC_{FP} . For ASRS, increasing the quantity of participating material around the ignition area tends to lower the LOC_{FP} . Previous work, which tested standard FM commodities, showed that the LOC_{FP} was dependent on the external packaging, with corrugated packaging resulting in lower LOC_{FP} values compared to plastics. As opposed to previous work, the ASRS testing included internal corrugated board within plastic containers. The internal packaging was shown to play a role in the LOC_{FP} by driving the ultimate value for LOC_{FP} over the external plastic material. The LOC_{FP} values of the internal contents generally aligned with values previously found for their respective standard commodities. For high-moisture-content frozen food applications, the external corrugated packaging material was the main driver for fire propagation. LOC_{FP} values were only slightly higher than those of standard corrugated products, benefiting from the low temperature of the food products stored within.

Acknowledgments

The author is grateful for the many contributions from several people that made this work possible. Firstly, the author would like to thank Jason Tucker, Sam Smith, and Dereck Mencarini of the Small Burn Laboratory at the FM Research Campus. They contributed greatly with the setup, execution, and cleanup of the tests. They also contributed input in the construction of the test apparatus to ensure feasibility, quick turnaround between tests, and maintained safety for the entire test campaign. Appreciation also goes to Kevin Mullins, George Nichols, and Janine Pitocco from the Research Campus for helping with hardware acquisition, scheduling, and to ensure that environmental health and safety was maintained during all parts of this project. Additionally, colleagues from Research, Xiangyang Zhou, Yibing Xin, Sergey Dorofeev, Benjamin Ditch, Gang Xiong, Franco Tamanini, and Yi Wang all provided useful feedback and discussion related to the experimental test plan, analysis, and recommendations during this work. Additional thanks to John LeBlanc from the Chief Engineer's Group of FM for providing valuable discussion in the implementation of ORS and feedback during all stages of this project. A special thank you to engineers at FM, Stephanie Arot, Harold Silbaugh, Michelle Blanchet, Keith Holzer, David Christensen, and Colin Berge, who provided information about frozen food storage to help guide the testing conditions of this commodity. Finally, the author would like to thank members of the Fire Protection Research Foundation technical panel and the Property Insurance Research Group for their valuable discussions and interactions during this project.

Table of Contents

Executive Summary.....	i
Abstract.....	iii
Acknowledgments.....	iv
Table of Contents.....	v
List of Figures	vi
List of Tables	ix
1. Introduction	1
2. Experimental Approach	4
2.1 Enclosure.....	5
2.2 Commodity Configurations	5
2.2.1 Mini-load Automatic Storage and Retrieval Systems (ML-ASRS).....	5
2.2.2 Frozen Food	9
2.3 Nitrogen and Air Supply.....	12
2.4 Instrumentation	13
2.5 Ignition Source	14
2.6 Success Criteria for Determining LOC	15
3. Results and Discussions	17
3.1 Mini-Load ASRS (ML-ASRS) Testing.....	17
3.1.1 Results for Different Containers	17
3.1.2 Impact of Internal Contents.....	28
3.1.3 Impact of Flue Space	30
3.2 Frozen Food Testing.....	34
3.2.1 Impact of Frozen Food Commodity	34
3.2.2 Impact of Moisture Content	38
4. Summary and Recommendations.....	39
References	41

List of Figures

1-1: Schematic of an oxygen reduction system.	1
1-2: Fire triangle for fire prevention and protection.	2
2-1: Elevation (a) and plan view (b) of test enclosure with air/N ₂ inlet pipe providing flow into a plenum under the storage area.	4
2-2: Elevation (a) and plan view (b) of the ML-ASRS storage configuration with 5-cm (2-in.) flue space.	6
2-3: Elevation (a) and plan view (b) of the ML-ASRS storage configuration with 15-cm (6-in.) flue space.	7
2-4: Corrugated box placed inside ML-ASRS container to evaluate effects on LOC _{FP} relative to empty containers.	8
2-5: Elevation (a) and plan view (b) of the frozen food rack storage arrangement with standard Class 3 corrugated boxes.	9
2-6: Elevation (a) and plan view (b) of the frozen food rack storage arrangement with wax-saturated boxes.	10
2-7: Elevation views of standard corrugated boxes (a) and wax-saturated boxes (b) showing the placement of the frozen food in green.	11
2-8: Internal packaging of frozen food meals within each a) standard corrugated box and b) wax-saturated box. The empty space in each box was filled with paper cups to prevent movement of the frozen food during setup. (Dimensions in in.)	11
2-9: Air and nitrogen supply system for the enclosure testing.	12
2-10: Oxygen concentration gas sampling and thermocouple locations for testing. (The two gas sampling locations with the storage bins were only used for ML-ASRS configurations.)	13
2-11: 33kW (31 BTU/s) premixed burner 0.3-m (1-ft) long and 2.5-cm (1-in.) wide placed within the central flue space. A V-shaped flame deflector above the burner diverts the flames towards the commodity on either side of the flue.	14
2-12: Parallel panel test configuration for surface heat flux evaluation of burner.	14
2-13: Surface heat flux measurements from igniter at four different parallel panel separation distances.	15
3-1: Images of fire development for solid-walled ML-ASRS at 16% O ₂ at selected times after ignition.	18
3-2: Images of fire development for solid-walled ML-ASRS at 15% O ₂ at selected times after ignition.	19
3-3: Chemical HRR for solid-walled ML-ASRS containers for a range of %O ₂ of 13-16%.	19
3-4: Measured (red) and calculated (blue) oxygen concentrations during 13% oxygen test.	20
3-5: Measured (red) and calculated (blue) oxygen concentrations during 15% oxygen test.	20
3-6: Sample images of color space transformation and resultant flame location as determined using Eqs. 3-1 and 3-2.	22
3-7: Flame height over time extracted from video for solid-walled ML-ASRS at 15% O ₂	23

3-8: Image highlighting the smoke profile extraction location along the vertical support riser.	23
3-9: Sample profile used to estimate the smoke layer height.	23
3-10: Smoke layer and flame height over time extracted from video for solid-walled ML-ASRS at 15% O ₂ . The black symbols represent flame height extraction based on visual observation of the videos.....	24
3-11: Overlay of smoke layer height (orange), measured oxygen concentration (blue) and the estimated oxygen at the top of the enclosure due to smoke (grey).	25
3-12: Images of fire development for vented ML-ASRS at 17% O ₂ at selected times after ignition.	25
3-13: Images of fire development for vented ML-ASRS at 16% O ₂ at selected times after ignition.	26
3-14: Chemical HRR for vented ML-ASRS containers in the range 15-17% oxygen.....	27
3-15: Overlay of smoke layer height (orange), measured oxygen concentration (blue) and the estimated oxygen concentration at the top of the enclosure due to smoke (grey). Oxygen was set to 16%.	27
3-16: Chemical HRR of the two ML-ASRS containers relative to UPP near their respective LOC _{FP}	28
3-17: Images of fire development for vented ML-ASRS with corrugated contents at 12% O ₂ at selected times after ignition.	29
3-18: HRR curves for ML-ASRS containers with internal corrugated cardboard contents at oxygen concentrations between 11 and 14%.	29
3-19: Post-test damage at 11% oxygen (a) and 14% oxygen (b) for the vented ML-ASRS with corrugated boxes within the containers.	30
3-20: Images of fire development for vented ML-ASRS with 15-cm (6-in.) flue space at 19% oxygen at selected times after ignition.	31
3-21: Images of fire development for vented ML-ASRS with 15-cm (6-in.) flue space at 18% oxygen at selected times after ignition.	31
3-22: Post-test damage showing sidewall melting (a) and pooling at the floor (b), following the vented container test with 15-cm (6-in.) flues and 18% oxygen.	32
3-23: HRR curves for ML-ASRS containers at a 15-cm (6-in.) flue space at various oxygen concentrations.	32
3-24: HRR curves for vented ML-ASRS containers at different oxygen concentrations with internal corrugated cardboard contents and a 15-cm (6-in.) flue space.	33
3-25: Post-test image of damage to the vented ML-ASRS containers and the internal corrugated boxes.	33
3-26: Images of fire development for frozen food in corrugated boxes at 13% oxygen at selected times after ignition.....	34
3-27: Images of fire development for frozen food in corrugated boxes at 14% oxygen at selected times after ignition.....	35
3-28: HRR curves for the frozen food fire testing using standard and wax-saturated corrugated packaging.	36
3-29: Post-test damage at the face of the second tier for frozen food stored in standard corrugated packaging, tests 1 (a) and 2 (b), and wax-saturated packaging (c) at 13% oxygen.	36
3-30: Damage to frozen food meal within first tier after the test at 13% oxygen.....	37

3-31: Measured oxygen concentration for each frozen food test. Increases were caused by the escape of atmospheric air within each box during the fire test. 37

3-32: Fire propagation probability by oxygen concentration estimated for cartoned commodities [3]. Brackets highlight the 0.5% delta between 67% and 5% fire propagation probability..... 38

List of Tables

2-1: ML-ASRS containers used in this study.....	8
3-1: Test configurations used for evaluation of the LOC_{FP} . Oxygen levels ranged between 11-18% vol.....	17
3-2: Measured moisture content of the corrugated cardboard packaging and the test results for each frozen food fire test.....	38
4-1: LOC_{FP} for ASRS and frozen food commodities tested in this work. Standard cartoned and uncartoned commodity values have been added for comparison.....	39

PAGE LEFT INTENTIONALLY BLANK

1. Introduction

An oxygen reduction system (ORS) is a fire prevention system that generates a low-oxygen environment to prevent ignition and limit fire propagation in a protected space. Figure 1-1 shows a schematic of an ORS with the components necessary to provide protection. The key element of an ORS is the nitrogen generator, which provides nitrogen that is pumped into the protected space, reducing its oxygen concentration. Sensors are used to monitor the oxygen level within the protected space, while the control unit adjusts the supply of nitrogen and air to maintain the desired conditions within the space.

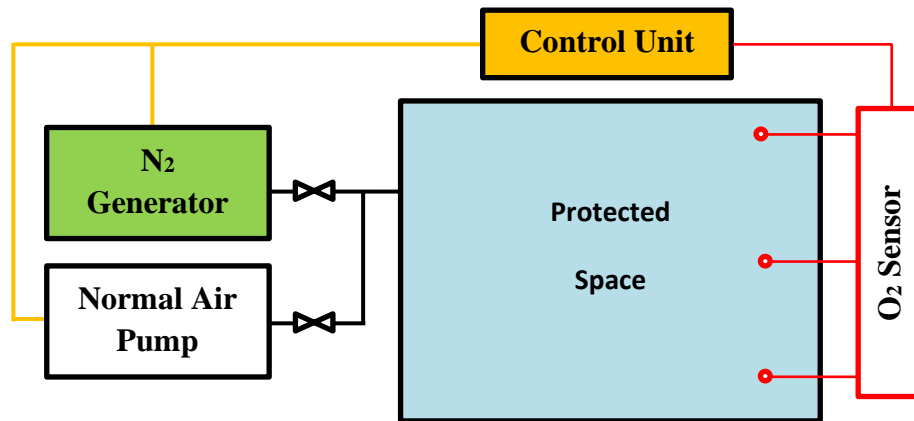


Figure 1-1: Schematic of an oxygen reduction system.

To understand how an ORS works, Fig. 1-2 shows the fire triangle, which highlights the three elements required to create and sustain a fire: combustible materials (fuel), oxidizer (O₂), and energy (heat) to initiate and sustain the exothermic chemical reaction. An ORS targets reduction of the oxidizer (i.e., the oxygen in ambient air) by displacing the oxygen with inert nitrogen. This results in lowering flame temperature (thermal ballast effect), increasing flame thickness and decreasing chemical reaction rates (diffusion transport and chemical kinetics effects). At sufficiently lower oxygen concentration the flame heat release rate drops below thermal and aerodynamic heat losses from the flame and combustion cannot be sustained. The subject of this study, however, is not the fundamental oxygen concentration for flame extinction outlined above, but instead involves understanding how the bulk oxygen concentration in a storage facility results in local conditions near the flame that would not support flame propagation, referred to in this work as the limiting oxygen concentration for fire propagation (LOC_{FP}). The LOC_{FP} is the maximum concentration of oxygen (oxidant) in a fuel-air (fuel-oxidant-diluent) mixture below which sustained fire propagation does not occur. This value is dependent on the ambient pressure and temperature, as well as ignition source and fuel characteristics. Note, that LOC_{FP} is generally larger than the fundamental extinction limit that can be observed locally near the flame.

If the ignition and/or fire propagation can be prevented, the damage from heat, water, and smoke becomes minimal, leading to better protection outcomes for high-value occupancies and other areas that are sensitive to those damage mechanisms. However, when the oxygen level drops below a certain threshold, e.g., < 19.5% by volume, safety becomes a concern even for a primarily unoccupied space [1].

Additionally, the cost of nitrogen production increases with lower oxygen requirements as longer purge times and flow rates are needed to maintain lower levels. Therefore, it is important to know what bulk oxygen level is required for protection. The limiting oxygen concentration for fire propagation (LOC_{FP}) is a key design parameter when using an ORS.

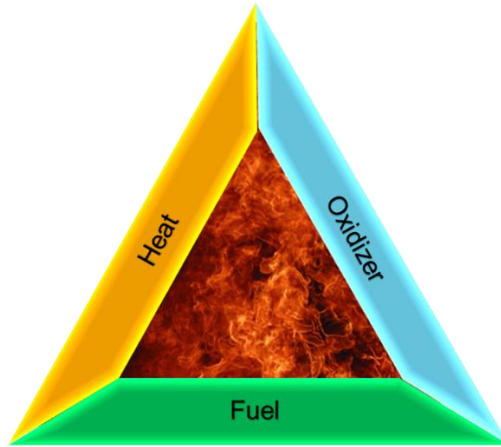


Figure 1-2: Fire triangle for fire prevention and protection.

The LOC_{FP} of many common fuels was studied using laboratory-scale experiments in previous work [2]. The results showed that the LOC_{FP} can be measured using a variable oxygen method in the Fire Propagation Apparatus (FPA). The measurements also showed that, for common fuels such as corrugated cardboard, wood, polystyrene (PS) and polyethylene (PE) plastic, the LOC_{FP} values are below 15%. If the ORS is designed properly, then the oxygen level will fall well below the safety limit of 19.5% [1]. As a result, safety is a real concern for the use of ORS.

Large- [3] and small-scale tests [4] have shown that the recommended oxygen levels for various commodities generally should be lower than those in existing standards from VdS, EU prEN, and ISO [5, 6, 7]. Previous research using both laboratory- and large-scale experiments has been conducted to determine LOC_{FP} values for standard materials and rack storage arrangements found within warehouses [2, 3]. These materials include Class 2, Cartoned Unexpanded Plastic (CUP), Cartoned Expanded Plastic (CEP), Uncartoned Unexpanded Plastic (UUP), and Uncartoned Expanded Plastic (UEP) commodities. The previous tests have formed the basis for the protection guidance in FM Data Sheet (FMDS) 4-13, *Oxygen Reduction Systems* [8].

This project was undertaken to expand our understanding of LOC_{FP} for commodities and configurations beyond the standard commodities used by FM. ORS manufacturers have been promoting the use of ORS for automatic storage and retrieval systems (ASRS) and frozen food storage. These two storage arrangements are of particular interest since they are normally unoccupied and are thus suitable for ORS. Both applications differ from previously tested FM standard commodities given their reduced flue space, unique container geometry, and/or higher moisture content. With these differences, it becomes important to understand any requisite changes to the LOC_{FP} .

In contrast to typical storage with cartoned commodities, an ASRS often consists of open-top plastic containers arranged with narrow flue space to maximize storage efficiency. Protection of an ASRS requires large water supply and possibly the use of in-rack sprinklers [9]. These requirements are the result of delayed water transport through the dense storage arrays, which challenges traditional ceiling-level sprinkler protection. The use of an ORS may provide a promising alternative strategy to achieve adequate protection for such applications. Toward that aim, this work establishes recommended LOC_{FP} values for a mini-load ASRS configuration.

ORS may also provide an alternative protection strategy for refrigerated storage where temperatures can be as low as -28°C (-18°F). Traditional wet-pipe sprinkler installations are avoided in this kind of storage due to the obvious challenge of preventing water within the pipes from freezing. Instead, dry-pipe or pre-action sprinkler systems can be used, but these systems are more costly, more complex, and less reliable [10]. The water supply is kept in a heated area, and a valve is opened to supply water to the piping in the event of a fire. A dry-pipe system within the freezer area must be kept pressurized with dry air to prevent ice plugs from forming that can block the supply of water. Additionally, the storage height must also be limited to ensure proper protection from the sprinklers. As storage heights increase and sprinkler installations become more challenging, an ORS may be a suitable protection solution since freezers are typically already unoccupied and well-sealed with a controlled atmosphere. However, the lower temperature and high moisture content of commodities stored in freezers relative to commodities in a standard warehouse may result in different LOC_{FP} . As such, potential changes in LOC_{FP} applicable to frozen food storage will be evaluated in this work.

2. Experimental Approach

This section describes the experimental setup used to represent a storage area with ORS protection. The setup was designed to represent conditions like those in a large facility where a quiescent controlled atmosphere surrounds the stored commodity. An enclosure was used to house the commodity and provide a desired air/nitrogen mixture with variable oxygen concentration. The following subsections describe the enclosure, the tested commodities, and the various support systems used to generate the conditions for testing fires in a reduced oxygen environment.

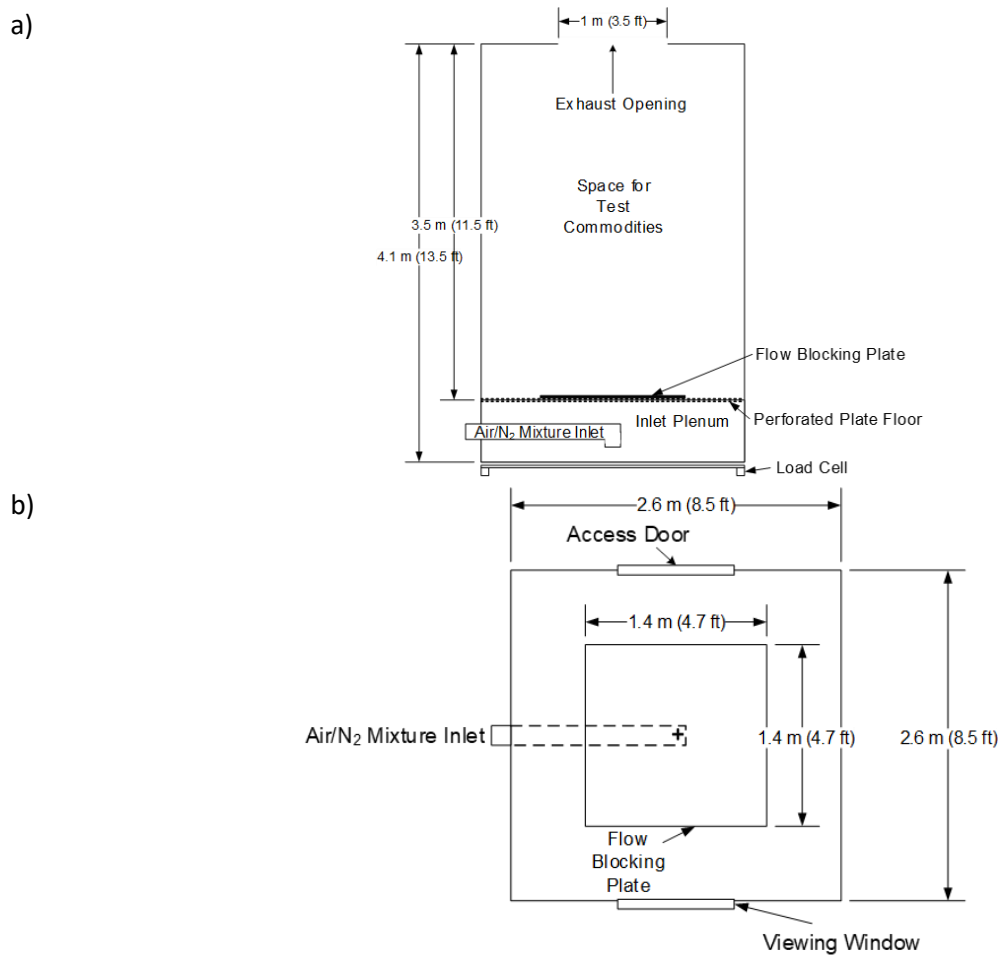


Figure 2-1: Elevation (a) and plan view (b) of test enclosure with air/N₂ inlet pipe providing flow into a plenum under the storage area.

2.1 Enclosure

The test enclosure was like that of previous work [3]. Figure 2-1 shows a schematic of the enclosure with two main areas: a test chamber to hold the tested commodity, and an inlet plenum where the reduced oxygen air mixture enters prior to flowing into the test chamber. The test chamber measured 3.5-m (11.5-ft) tall with a 2.6-m (8.5-ft) square footprint. The air/nitrogen mixture flowed from the inlet plenum through a perforated plate, 3.2-mm (1/8-in.) thick, with 30% open area, before entering the test chamber. This perforated plate provided a pressure drop that helped to create a uniform flow distribution into the chamber. Flow uniformity was tested using a sonic anemometer (Campbell Scientific, CSAT3) with variation of 10% measured around the commodities. A blocking plate, 3.2-mm (1/8-in.) thick, was placed in the center of the chamber to shield the commodity from the flowing gas mixture. As shown in previous work, this blocking plate had little effect on the LOC_{FP} , and helped to simulate a large warehouse with a solid floor, where only the surrounding reduced-oxygen gases would participate in a fire with no oxygen replenishment directly beneath the commodity.

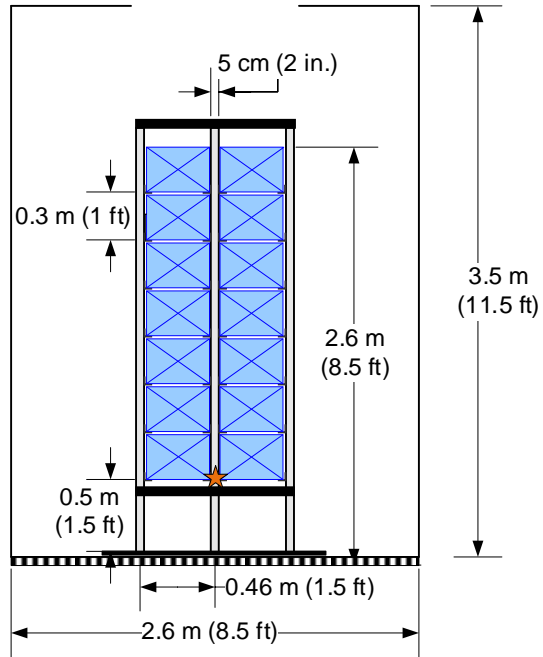
An exhaust opening allowed gases to escape the chamber. The combustion products were collected in a 5-MW calorimeter and used to measure the chemical heat release rate (HRR) during each test. An access door was used for setup, extinguishment, and cleanup of any tests performed. The viewing window provided optical access for photo and video documentation. The doors, windows, and walls were all sealed to ensure minimal leakage of the supplied gasses from within the enclosure to the surrounding laboratory area.

2.2 Commodity Configurations

2.2.1 *Mini-load Automatic Storage and Retrieval Systems (ML-ASRS)*

When compared to the standard storage configurations tested previously, ASRS consists of more closely spaced commodities with smaller flue spaces. These result from the use of industrial robots and automated pullers to handle storage containers. The robots operate more precisely than fork truck operations and thus storage bins can be placed closer for more efficient use of space. The mini-load ASRS (ML-ASRS) style configurations tested are shown in Figs. 2-2 and 2-3. Both configurations used 7-tier 2x2 arrays of containers providing enough height to evaluate flame propagation in the reduced oxygen environment. The first configuration in Fig. 2-2, represents a smaller 5-cm (2-in.) flue space, while the second in Fig. 2-3, represents larger 15-cm (6-in.) spacing. The smaller flue space condition covers the spacing found in an actual ML-ASRS arrangement (8-cm [3-in.]). The small flue spaces are also representative of those in other types of ASRS such as top-load ASRS. It is expected that the results and observed trends from this work can be applicable to other such densely packed storage arrangements. The larger 15-cm (6-in.) spacing was selected to compare the performance of identical commodity with a spacing found in traditional rack storage. Tests were ignited within the flue space at the bottom tier of storage. The first tier was elevated from the floor at 0.5-m (1.5-ft), as is typical in an ASRS.

a)



b)

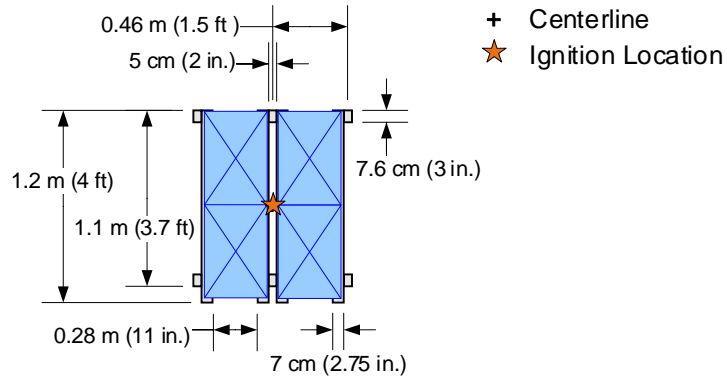


Figure 2-2: Elevation (a) and plan view (b) of the ML-ASRS storage configuration with 5-cm (2-in.) flue space.

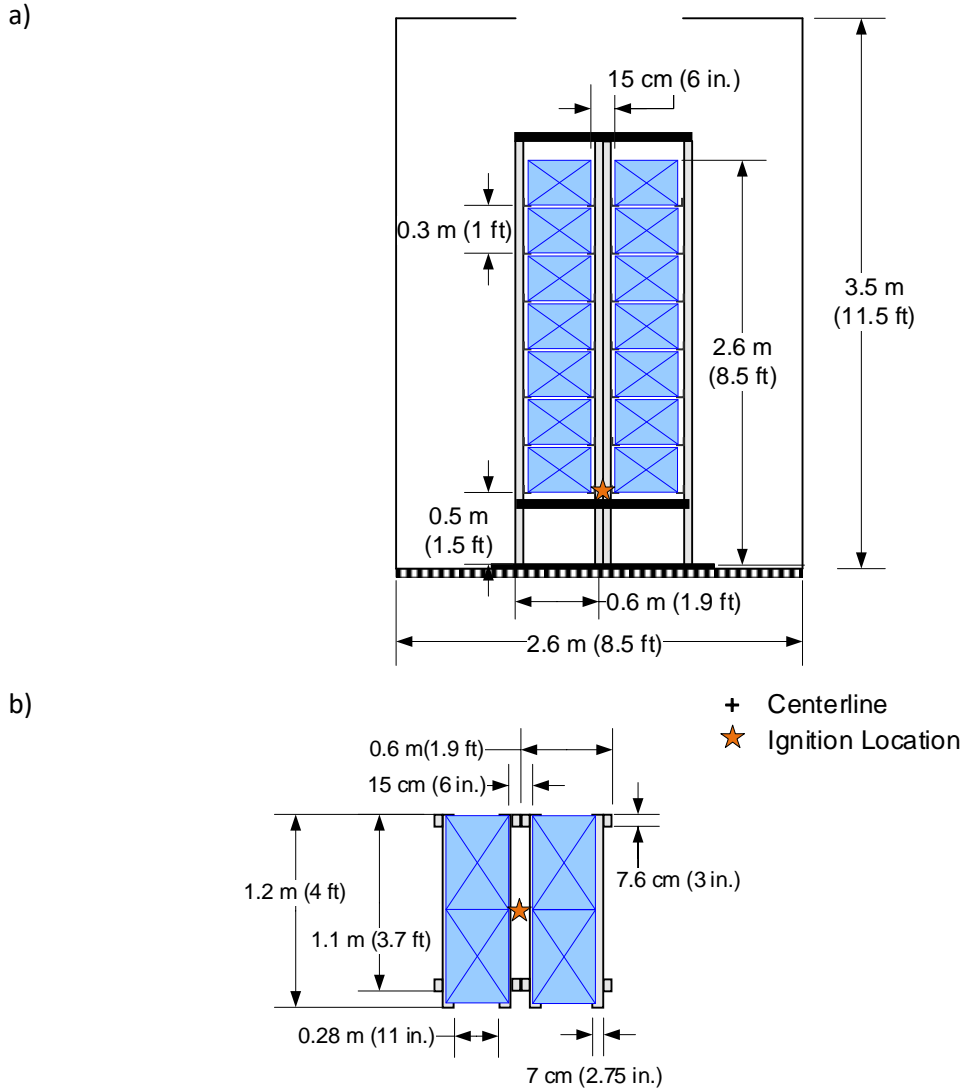




Figure 2-3: Elevation (a) and plan view (b) of the ML-ASRS storage configuration with 15-cm (6-in.) flue space.

There is a large assortment of containers used in ML-ASRS. They may have varying wall thicknesses, different sizes, solid or vented walls, and may be collapsible. Two different containers were selected for testing with the intent of bounding how much the LOC_{FP} may change depending on varying container characteristics (see Table 2-1). A solid-walled container was used to represent a high-mass container with thick walls and no vents. A vented-wall container with lower mass and thinner side walls was tested for comparison. Both containers were made of a polypropylene copolymer with material properties similar to those of polypropylene (PP).

Table 2-1: ML-ASRS containers used in this study.

Type (Style)	Dimensions mm (in.)	Mass kg (lbs)	Image
Solid wall (Unvented)	595 × 395 × 280 (23.4 × 15.6 × 11.1)	4.4 (9.7)	
Vented wall (Collapsible)	600 × 400 × 285 (23.6 × 15.7 × 11.2)	3.3 (7.2)	

ASRS containers are used to store many different types of products. From previous studies, the LOC_{FP} for standard commodities differed depending on the tested external packaging material: cartoned and uncartoned commodities measured 11.1% and 13.0% LOC_{FP} , respectively [3]. In the event of a fire, the relatively thin walls of the ASRS containers will likely melt or burn out, exposing whatever internal contents are present to the flame. To capture possible variations in the LOC_{FP} , tests were conducted with empty containers and ones with corrugated board contents. The combination of plastic external packaging and corrugated internal packaging has not been tested in the past. The empty containers represent a condition where minimal combustible material is stored. Fire growth would then be driven by the combustible material of the containers themselves. On the other hand, stored cartoned commodities, which alone have an LOC_{FP} lower than that of uncartoned plastics, may drive additional fire growth affecting the LOC_{FP} . The stored contents, placed within each container, consisted of a corrugated box filled with paper cups made to fit within the containers (see Fig. 2-4), representing an intermediate level of fire hazards typical to ASRS applications.



Figure 2-4: Corrugated box placed inside ML-ASRS container to evaluate effects on LOC_{FP} relative to empty containers.

2.2.2 Frozen Food

Storage conditions in freezers vary greatly from those in a standard warehouse, with temperatures below the freezing point of water and relative humidity (RH) levels around 100%. Stored contents also have high moisture content at low temperatures representing a substantial thermal sink relative to standard warehouse commodities. In freezer conditions, standard corrugated cardboard may become weak and fail [11]. To prevent this, typical freezer packaging is protected from moisture by using various approaches. Corrugated packaging can be wrapped with a thin plastic film or coated with wax to prevent moisture absorption from the freezer environment. Plastic packaging can also be used, but the plastic itself would not be altered by the conditions in the freezer and the known LOC_{FP} values of UUP and UEP could provide guidance for those commodities [2]. Therefore, the focus of the present study was to understand the LOC_{FP} of low-temperature cartoned commodities with frozen food inside.

This work used a two-tier rack fuel array supporting four half pallets loads of frozen food commodity. The rack itself was set up inside the enclosure with a 1 x 1.3-m (3.5 x 4.2-ft) footprint. Wooden half pallets were placed on the racks with a 0.15-m (6-in.) flue space between pallets. Two different frozen food packaging materials were placed on the racks. The first tested was standard corrugated cardboard with a plastic film with the arrangement shown in Fig. 2-5. The plastic film was not expected to contribute to fire growth as it would either quickly burn off or shrivel away, leaving just the cardboard layer exposed to flames. The film, however, served to protect the low-temperature corrugated cardboard from absorbing moisture. The boxes were all conditioned to a moisture content range found in a typical freezer prior to testing (7-13% by weight measured on a dry basis).

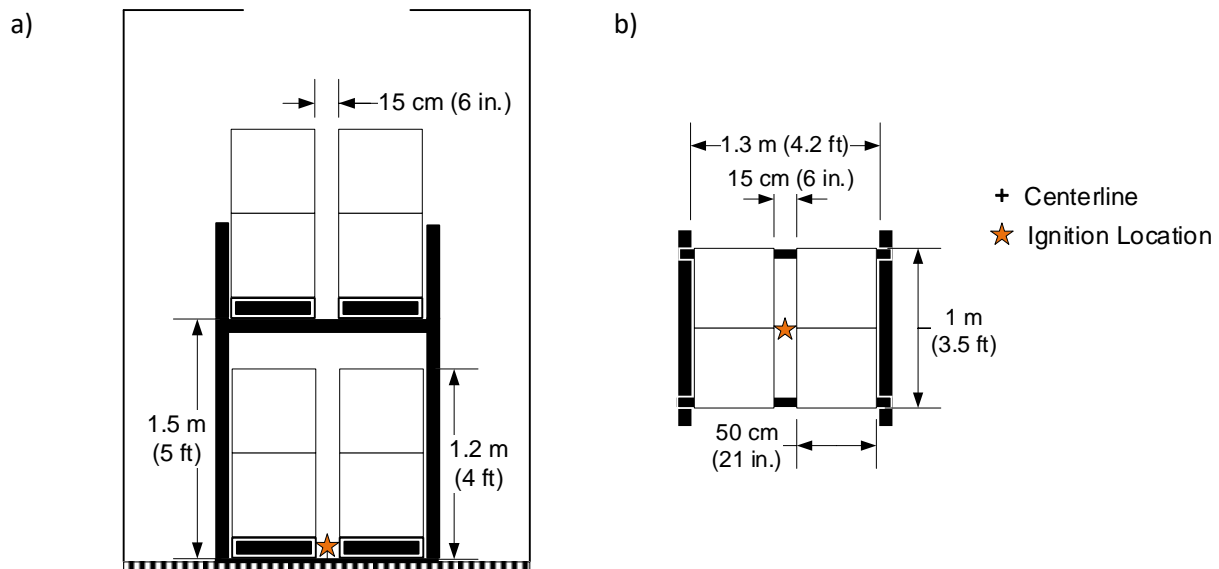


Figure 2-5: Elevation (a) and plan view (b) of the frozen food rack storage arrangement with standard Class 3 corrugated boxes.

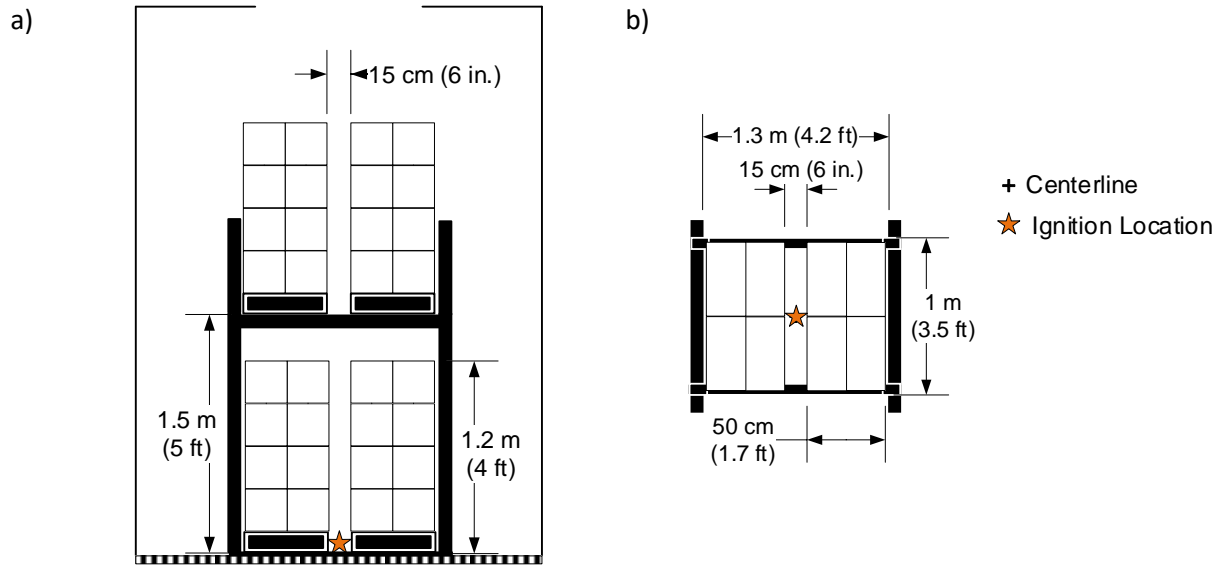


Figure 2-6: Elevation (a) and plan view (b) of the frozen food rack storage arrangement with wax-saturated boxes.

The second packaging material tested was wax saturated corrugated boxes, the arrangement is shown in Fig. 2-6. These are used in storage environments where moisture control becomes an issue or contents require ventilation to prevent the food from spoiling. In those cases, the boxes cannot be wrapped in plastic. The wax provides a barrier against moisture absorption from both the external environment and internal contents. As wax is composed of hydrocarbons, the coatings may affect the burning behavior of the commodity. A single test using wax boxes was performed to evaluate differences from the standard corrugated board.

Food stored within freezers can vary greatly, with differences in water content and inclusion of other materials for containment. Prepackaged frozen food meals were selected to represent frozen commodities within these storage arrangements. Frozen meals, such as dinners and pizzas, represent a large portion of frozen food sold by the food industry [12, 13], second only to ice cream. As opposed to ice cream, frozen meals contain additional packaging materials consisting of foils and plastics, which contribute to increased fuel loading and may promote fire growth. The frozen dinners tested consisted of food contents in a plastic tray sealed using cellophane film. The plastic tray was housed inside a cardboard box. It is expected that testing with the frozen dinners would be applicable to other frozen goods, where food is packaged with small amounts of plastic in cardboard box. For example, a typical frozen pizza is wrapped in cellophane and placed in a cardboard box similar to a dinner package without the plastic tray. When frozen, these meals can represent a significant thermal sink against sustaining fire growth. Water content of the frozen food is typically high, with about 80% of the food mass as frozen water. Still, it was expected that the fire growth for frozen food should behave similarly to the cartoned commodities tested in the past [3].

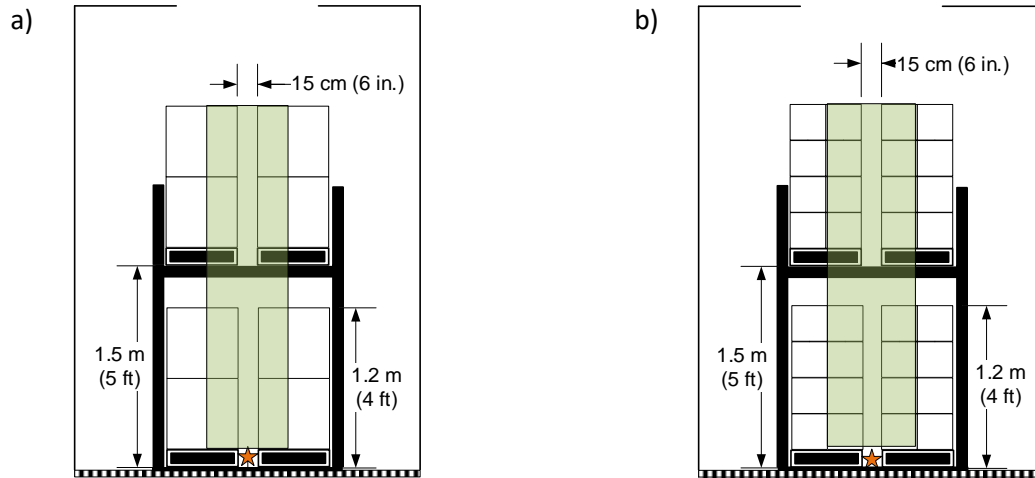


Figure 2-7: Elevation views of standard corrugated boxes (a) and wax-saturated boxes (b) showing the placement of the frozen food in green.



Figure 2-8: Internal packaging of frozen food meals within each a) standard corrugated box and b) wax-saturated box. The empty space in each box was filled with paper cups to prevent movement of the frozen food during setup. (Dimensions in in.)

In the present work, frozen food was placed in the containers surrounding the central flue space, (see Fig. 2-7), as it was expected the primary fire growth would be within that space above the ignition location, with generally slower horizontal spread. Standard-sized frozen meals from Stouffers were placed within each corrugated box and arranged such that the meal was in contact with the surface nearest the central flue (see Fig. 2-8). The remaining space within each box was filled with paper cups to prevent the frozen food from shifting before or during the test. As will be shown later in the results, this quantity and arrangement of frozen food was suitable, and the fire never reached the paper cups within each box.

Testing low-temperature products representing actual freezer storage applications was a key element of understanding the LOC_{FP} of frozen food. In a freezer, both the surrounding air and the products are at low temperatures, -17 to -28 °C (1.4 to -18 °F). It has been estimated that the temperature of the fuel (food in this case) has a greater effect on LOC_{FP} than the surrounding air temperature. Indeed, previous testing has shown that ambient temperature effects on the LOC_{FP} are minimal with a 0.5% increase in LOC_{FP} from 20 °C to -20 °C (68 °F to -4 °F) [2]. Modeling of polymethylmethacrylate (PMMA) material using the theoretical approach found in Ref. [2], but with heat loss (as in heat loss to the frozen food),

showed that the LOC_{FP} can change by 2% depending on the external heat flux level. Furthermore, the amount of energy required to heat air compared to the frozen food is also different, driven by the specific heat and density differences of ice and air. As an example, it would take approximately 3 minutes to heat 0.03 - 0.06 m³ (1-2 ft³) of frozen food from -20 °C to 0 °C (-4 °F to 32 °F) with 6-12 kW (5.7 – 11.4 Btu/s) of power (*i.e.*, an oxy-acetylene torch). Bringing the food to combustion temperatures would also require the additional energy required for phase change. The time scales drive the need for extended ignition times over 3 minutes when evaluating possible fire growth in reduced oxygen conditions. Based on these estimates, the entire fuel array (food, boxes, plastic film, and pallets) was brought to -18°C (0°F) prior to ignition. The air was not cooled as minimal heating of the commodity in ambient air is expected during the test (the igniter will provide the main source for initial heating).

2.3 Nitrogen and Air Supply

A mixture of air and nitrogen was injected into the enclosure to purge the ambient air and set the desired oxygen concentration. Figure 2-9 shows the piping and components used to generate and transport the required gas mixture to the enclosure. A blower motor forced the necessary flow of gas into the inlet of the enclosure. A liquid nitrogen tanker was placed outside of the laboratory and nitrogen gas was injected upstream of the blower fan and mixed within the fan and through the duct. Injection of nitrogen prior to the blower motor allowed for independent adjustment of both oxygen concentration and total flow rate.

An orifice plate was installed to measure the flow through the inlet pipes. The plate, measuring 18.4 cm (7.25 in.) in diameter was placed within the long pipe section used to transport the gasses to the enclosure. Pipe lengths upstream and downstream of the orifice plate were a minimum of 5.5 m (18 ft) and 1 m (3.5 ft), respectively, to achieve accurate flow measurements based on ISO 5167-2 [14]. A fixed total flow rate of 0.61 m³/s (1300 CFM) was set to provide enough oxygen to support a 1-2 MW fire. Different flow rates in the range 0.33 -1.0 m³/s (700-2000 CFM) were tested previously, and a negligible effect was found on the LOC_{FP} [3]. A feedback controller connected to the blower motor (Dayton 3C107A) ensured a constant flow rate as designed. Nitrogen flow measurements were provided by a mass flow meter (Invensys CFT51).

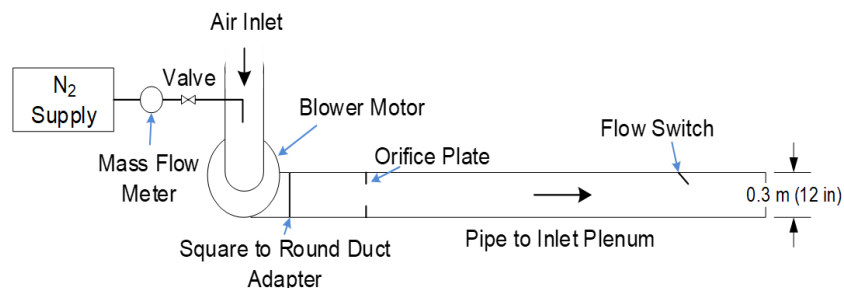


Figure 2-9: Air and nitrogen supply system for the enclosure testing.

A mixture of air and nitrogen was also injected into the ASRS containers for a duration of 1-2 minutes prior to ignition. This ensured the conditions within each container matched those in the surrounding

air. A secondary system of tubing was connected to the inlet pipe using a butterfly valve to only provide flow when necessary. The valve was closed prior to ignition and for the duration of each test. Purging of the frozen food packaging was not performed as frozen foods would have sealed ambient air within the packaging. Additionally, timescales for the internal conditions to match the exterior low oxygen concentrations are expected to be much longer than the turnover rate of food in a facility. Furthermore, the possibility of new products entering a warehouse suggests that internal conditions for product will resemble standard oxygen concentrations.

2.4 Instrumentation

Temperature and oxygen concentrations were measured at various locations within the enclosure (see Fig. 2-10). Temperature measurements within the array were added for assessments of fire growth and test failure if visibility of the flames became an issue through the viewing window. A thermocouple tree placed within the flue space consisted of six grounded 1.5-mm (0.062-in.) K-type thermocouples with 0.3-m (1-ft) spacing, with the first thermocouple placed 0.6 m (2 ft) above the ignition location. Fuel surface thermocouples were added to the top of the uppermost container near the flue space. The surface thermocouples provided a secondary metric for termination of the test by indicating whether the top of the fuel array was burning.

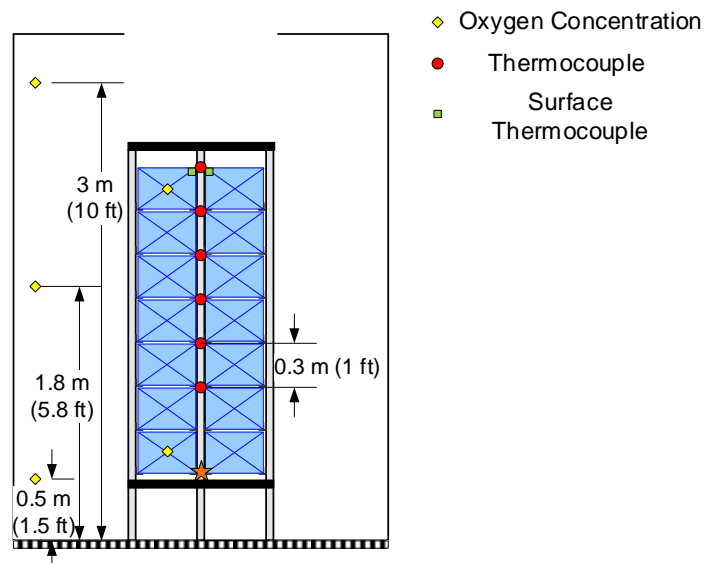


Figure 2-10: Oxygen concentration gas sampling and thermocouple locations for testing. (The two gas sampling locations with the storage bins were only used for ML-ASRS configurations.)

Oxygen concentrations were measured at three locations: 0.5, 1.8, and 3 m (1.5, 5.75 and 10 ft) from the floor. Following initial checks for gas uniformity within the enclosure, the three locations were averaged into one measurement for oxygen concentration within the enclosure. Figure 2-10 shows two additional oxygen concentration measurement locations within the storage containers. These data were used for characterizing the time required to purge the ambient air from all ASRS containers. They were not used during fire testing due to limited instrumentation available for gas analysis. Initial evaluations

showed that 02:30 (min:s) of purge flow was required to balance the oxygen concentration in the ASRS containers with that of the surrounding air prior to ignition for each test.

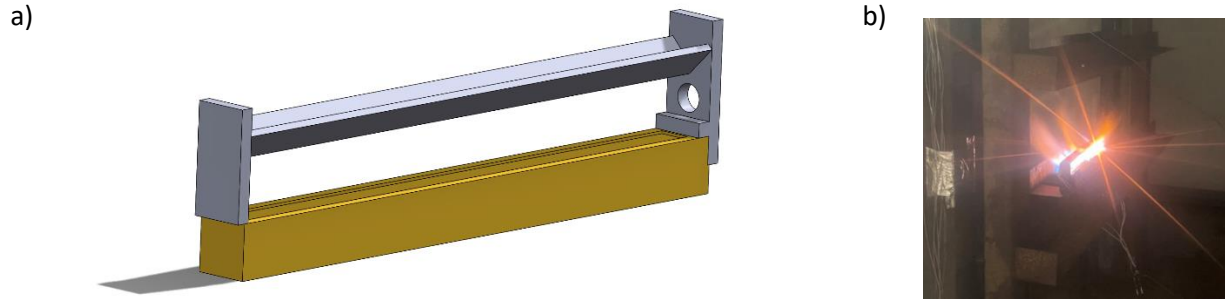


Figure 2-11: 33kW (31 BTU/s) premixed burner 0.3-m (1-ft) long and 2.5-cm (1-in.) wide placed within the central flue space. A V-shaped flame deflector above the burner diverts the flames towards the commodity on either side of the flue.

2.5 Ignition Source

An ignition source for the fire test was selected to provide uniform heating to the commodity regardless of the enclosure oxygen condition while also fitting within the small flue spaces present in ASRS storage. A premixed propane/air flame, with a chemical HRR of 33 kW (31 BTU/s) provided ignition performance similar to that of the FM standard igniters used for typical large-scale fire tests. Propane at 22 LPM (0.78 CFM) and air at 380 LPM (13.4 CFM) were combined within a venturi mixer prior to entering the burner. A 2.5 cm (1 in.) wide and 0.3 m (1 ft) long ribbon burner manufactured by AGF [15] was fit into the central flue space in all tests (see Fig. 2-11a). A V-shaped flame deflector placed above the burner ensured the flame would be aimed towards the commodity surfaces on either side of the flue. Ignition was controlled remotely with two hot surface igniters placed on each end of the burner. The flame created by the V-shaped deflector and ribbon burner is shown in Fig. 2-11b, with a uniform flame sheet exiting the burner on each side.

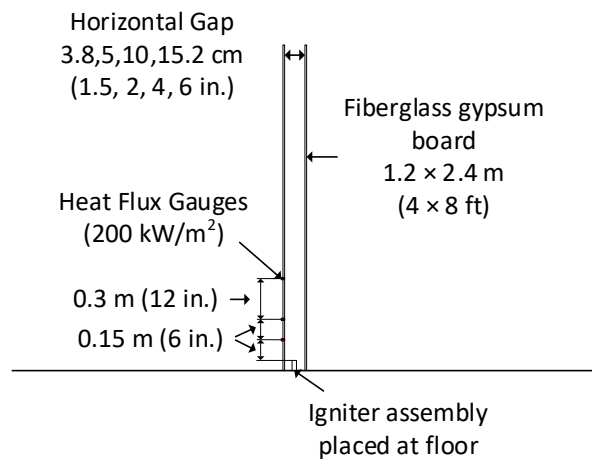


Figure 2-12: Parallel panel test configuration for surface heat flux evaluation of burner.

The ignition source was evaluated to ensure that similar surface heat fluxes could be generated for the flue spaces tested in this study (5-15 cm [2-6 in.]). This was important since the heat flux has been found to affect the oxygen concentration at which flaming and smoldering can occur [16]. An instrumented parallel-panel test was performed using Gardon-type heat flux gauges at various distances from the burner surface (see Fig. 2-12). The panel separation was varied among 3.8, 5, 10, 15 cm (1.5, 2, 4, and 6 in.) to observe similarity near the burner. As shown in Fig. 2-13, the surface heat flux was found to be within 7% at a distance of 15 cm (6 in.) from the burner. The flux varied significantly higher up the vertical panels; however, similarity within the ignition area was of most importance.

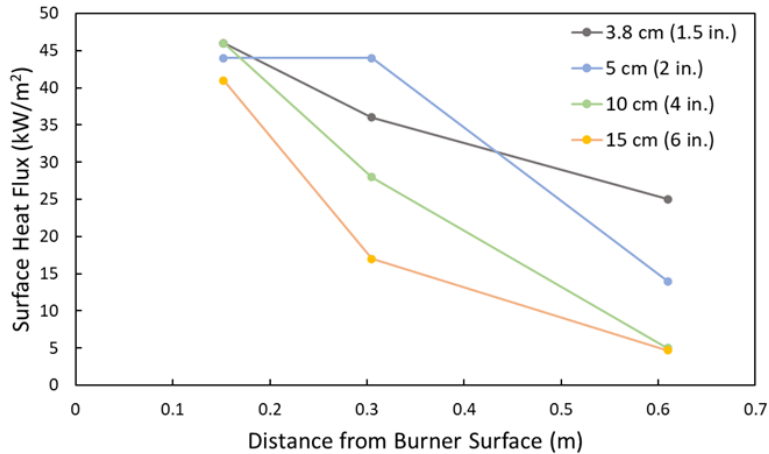


Figure 2-13: Surface heat flux measurements from igniter at four different parallel panel separation distances.

2.6 Success Criteria for Determining LOC

Protection success in each test was assessed using an ignition duration which provided enough time to evaluate fire propagation in conditions of sustained ignition. An ignition duration of 10 minutes was chosen based on the fire growth observed during previous large-scale tests and provided a duration representative of a sustained ignition scenario (credible worst-case scenario). The LOC_{FP} was defined such that when the oxygen level in the enclosure was at or below the LOC_{FP} , limited fire propagation must be observed throughout the 10-minute ignition period. A shorter duration (*e.g.*, 3 minutes) would not provide enough time for evaluation of fire growth changes with reduced oxygen. In those cases, materials such as plastics require more time for fire growth even at standard atmospheric oxygen concentrations.

The success criteria for establishing an LOC_{FP} were defined as follows:

- Igniter on for 10 minutes.
- If the fire does not reach the top of the test array – protection success and the LOC_{FP} for sustained ignition should be equal to or greater than the set oxygen level.
- If the fire reaches the top of the array – protection failure for sustained ignition scenario and the LOC_{FP} should be lower than the set oxygen level.

In the event of protection failure, the possibility of a “soft” LOC_{FP} in scenarios without sustained ignition was also evaluated:

- If the fire reduces in size after igniter shut-off – the soft LOC_{FP} should be equal to or greater than the set oxygen level.
- If the fire persists or grows for 30 seconds after igniter shut-off – the soft LOC_{FP} should be lower than the set oxygen level.

The purpose of this work primarily focused on determining the LOC_{FP} for sustained ignition and reported values reflect those conditions. Complementary information pertaining to the soft LOC_{FP} are pointed out throughout the results, but in many cases the values may be higher than what was tested in this work.

3. Results and Discussions

In this section, test results for the ML-ASRS configurations are summarized in Sec. 3.1. Results for ML-ASRS highlight changes in LOC_{FP} among differences in the container geometry, flue space, and internal contents. Additionally, results from the frozen food commodities are summarized in Sec. 3.2. The number of tests conducted in each configuration is shown in Table 3-1 with results from each set used to estimate an applicable LOC_{FP} .

Table 3-1: Test configurations used for evaluation of the LOC_{FP} . Oxygen levels ranged between 11-18% vol.

Configuration Number	Commodity	Contents	Flue Space	# of Tests
1	Solid ML-ASRS	Empty	5 cm (2 in.)	5
2	Solid ML-ASRS	Corrugated Board with Paper Cups	5 cm (2 in.)	1
3	Solid ML-ASRS	Empty (No purge)	5 cm (2 in.)	1
4	Vented ML-ASRS	Empty	5 cm (2 in.)	4
5	Vented ML-ASRS	Corrugated Board with Paper Cups	5 cm (2 in.)	4
6	Solid ML-ASRS	Empty	15 cm (6 in.)	2
7	Vented ML-ASRS	Empty	15 cm (6 in.)	3
8	Vented ML-ASRS	Corrugated Board with Paper Cups	15 cm (6 in.)	2
9	Class 3 with Frozen Food	Frozen Food /Paper Cups	15 cm (6 in.)	4
10	Wax-saturated Corrugated Boxes with Frozen Food	Frozen Food /Paper Cups	15 cm (6 in.)	1
Total Tests				27

3.1 Mini-Load ASRS (ML-ASRS) Testing

3.1.1 Results for Different Containers

Two different ML-ASRS containers were tested to evaluate the effect of geometry on the fire propagation and ultimately the LOC_{FP} . Testing of the solid-walled ML-ASRS containers with oxygen levels ranging from 13 to 16% provided an initial observation at the fire development. Figure 3-1 illustrates the fire growth for solid-walled containers with a 5-cm (2-in.) flue space and an ambient oxygen concentration of 16%. The fire development is illustrated in the five snapshots in Figure 3-1 at the selected times following ignition. During the first 45 s of each test, the fire is primarily within the flue space and grows up the side walls of the containers. At the 90 s mark, fire within the flue space reaches about half-way up the test array. There is a lateral broadening of the flame volume in the first

tier as the walls of the containers burn or melt away, exposing additional container surfaces to the fire. Once the container walls along the bottom tiers burn away, about 180 s, the fire grows from within each container instead of within the flue space. The fire continues to grow in size, moving up subsequent containers. Around 300 s, flames in the containers of the first 4 tiers are visible and burning of melted and dripped plastic can be observed at the floor level. At this oxygen concentration the fire size grows uncontrollably. The igniter was turned off at 350 s. Following igniter shutdown, the fire continued to grow with flames eclipsing the top of the array at 390 s. Under these conditions, test results clearly indicated ORS protection failure, and that a lower oxygen concentration was needed to provide adequate protection against fire propagation.

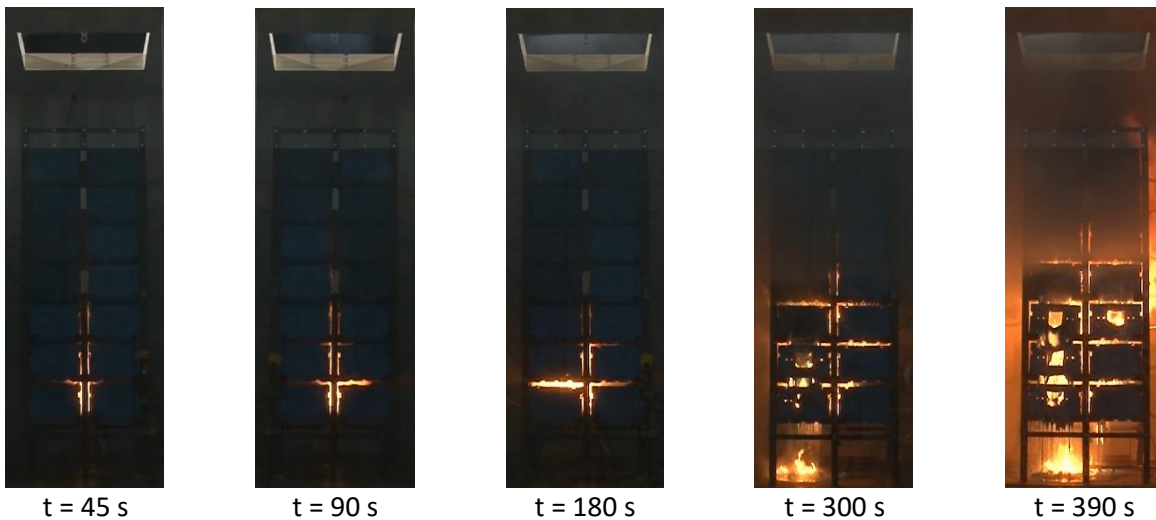


Figure 3-1: Images of fire development for solid-walled ML-ASRS at 16% O₂ at selected times after ignition.

A decrease in the ambient oxygen concentration by one percent (to 15%) caused a notable difference in the fire development, as shown by the snapshots in Fig. 3-2. Initially, fire growth was identical to that observed in the 16% oxygen concentration test. Burning was initially limited to within the 5-cm (2-in.) flue space, but around 180 s, the fire settled into the containers. The fire grew slowly, eventually reaching the bottom of the fifth tier. In contrast to the test at 16% oxygen level, a smoke layer within the enclosure formed at about 300 s, and at 360 s the fire size decreased. Plastic continued to melt and burn at the floor level during the test. The fire size continued to decrease and, ultimately, settled around the first tier where the fire from the igniter was easily visible due to consumption of the surrounding material. The results indicated successful ORS protection with fire propagation limited to the storage array over the 10-minute test duration. The effects of the smoke layer on the local oxygen concentration were investigated later to understand whether locally reduced oxygen concentration influenced the limited fire growth.

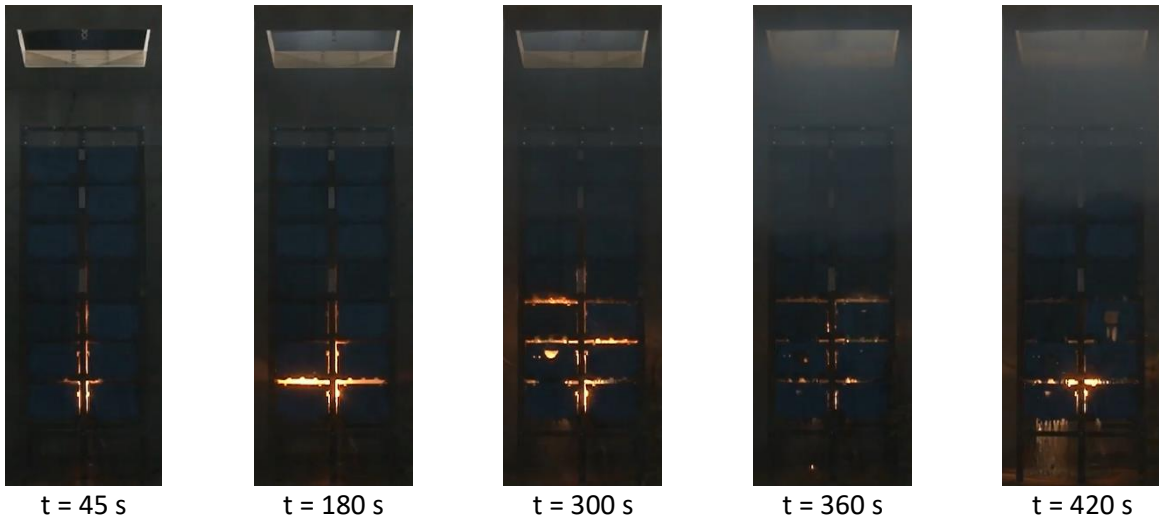


Figure 3-2: Images of fire development for solid-walled ML-ASRS at 15% O₂ at selected times after ignition.

Chemical HRR data show the different fire growth trends for the solid-walled ML-ASRS tests (see Fig. 3-3). At 16% oxygen, fire growth was uncontrolled before and after igniter shutoff. The HRR reached approximately 1 MW and manual extinguishment was required to suppress the fire. At 15% oxygen, the HRR stabilized at approximately 100 kW for a period of one minute prior to decreasing. Tests at 13-15% oxygen also indicated ORS protection success with limited fire propagation under sustained ignition.

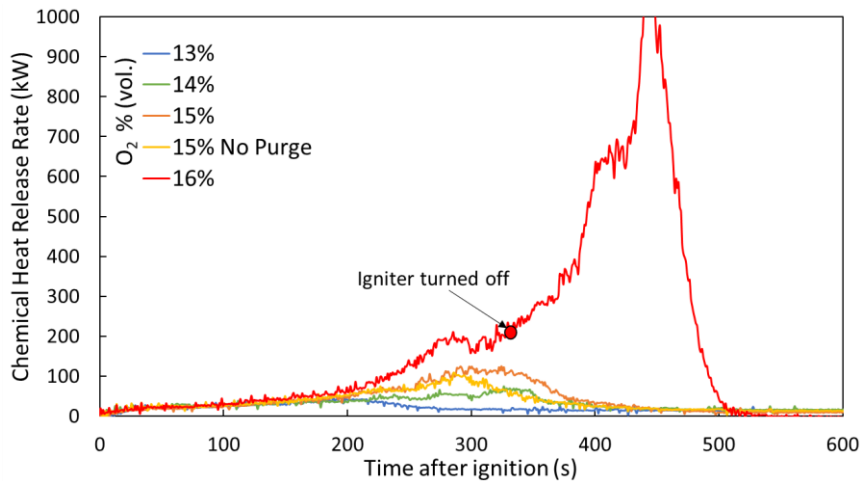


Figure 3-3: Chemical HRR for solid-walled ML-ASRS containers for a range of %O₂ of 13-16%.

A second test at 15% oxygen with no purging of the containers was also successful. The purge gas thus had a negligible effect on the fire growth as the gaps between the containers provided adequate openings for gas flow between the containers and surrounding environment. A sealed container initially filled with normal air, however, could provide a local source of oxygen to promote fire growth, thus results here are applicable for open-top containers only.

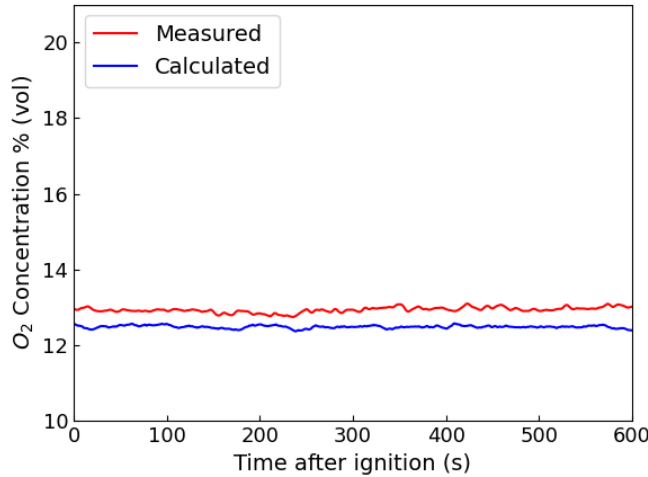


Figure 3-4: Measured (red) and calculated (blue) oxygen concentrations during 13% oxygen test.

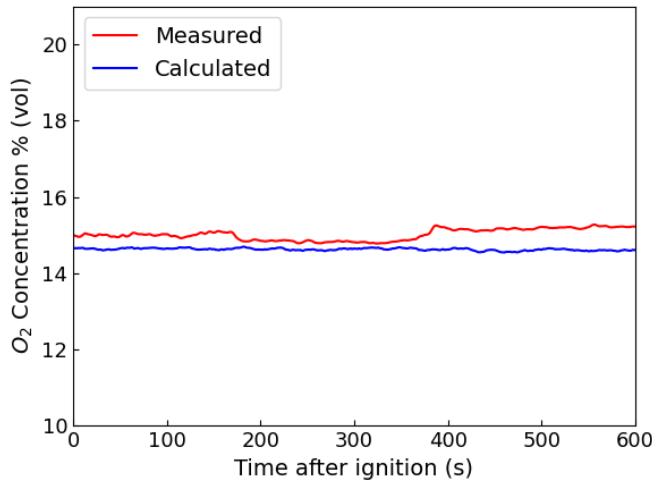


Figure 3-5: Measured (red) and calculated (blue) oxygen concentrations during 15% oxygen test.

Oxygen concentration measurements were analyzed to ensure stable levels were maintained during each test. Figure 3-4 shows both the measured oxygen concentration from within the enclosure and a calculated oxygen level based on instrumentation within the inlet duct for the test at 13% oxygen. Both values are stable with the offset attributed to uncertainties in the mass flow and temperature readings in the duct used for calculating the volumetric flow of nitrogen. The measured oxygen concentration within the enclosure was used for setting flows within the enclosure and evaluating the LOC_{FP} . Calibration of the calculated values to the measured values would bring them in line; however, the measured values provide a look into gas concentration behavior entering the enclosure. Figure 3-5 shows oxygen readings for the 15% O₂ case. Here, a temporary decrease in the measured value can be seen from 200 to 400 s. During the early stages of smoke development there is no physical overlap between the smoke layer and the location of the flames. However, towards the end of this 200 s smoke period, the layer becomes thicker and starts to overlap spatially with the location of the flame front. Based on this result, it is expected that the smoke layer present at the top of the enclosure extended

down far enough to reach the uppermost gas sampling location (see Fig. 2-11), affecting the measured oxygen level toward a slightly lower value.

The successful protection demonstrated for the test at 15% oxygen was deemed to be due to the local drop in oxygen concentration in the upper part of the enclosure. In this area the smoke serves as an additional source of dilution further lowering oxygen concentration. The contribution of smoke, and combustion products, to the nitrogen only represents a small percentage of the gas mixture, ≈1% in addition to the setpoint of 85% nitrogen, and thus differences in properties are negligible. The test video was analyzed to extract both the flame and smoke layer height to demonstrate overlap in fire growth relative to the presence of the smoke layer. The flame height was determined by converting the RGB color map to an YCrCb intensity map representing luminosity (Y), difference in red (Cr) and difference in blue (Cb). This approach has been used successfully in the past for video detection of fires [17, 18]. Conversion of the colors pace to YCrCb was performed using Eq. 3-1,

$$\begin{bmatrix} Y \\ Cb \\ Cr \end{bmatrix} = \begin{bmatrix} 0.2568 & 0.5041 & 0.0979 \\ -0.1482 & -0.2910 & 0.4392 \\ 0.4392 & -0.3678 & -0.0714 \end{bmatrix} \begin{bmatrix} R \\ G \\ B \end{bmatrix} + \begin{bmatrix} 16 \\ 128 \\ 128 \end{bmatrix}. \quad 3-1$$

Using the converted colormap, the presence of the flame within each video frame is defined by the conditions shown in Eq. 3-2,

$$\begin{matrix} Cr > Y \times \mu \\ Cr > Cb \end{matrix} \rightarrow \text{flame}. \quad 3-2$$

An attenuation factor, μ , in Eq. 3-2 was used to capture the lower luminous flames present within the flue space during the test. This inclusion can increase the likelihood of false positives when used for flame detectors. However, a value of 0.6 was found to be suitable to best estimate flame height relative to the RGB images.

Sample images of the various color components are shown in Fig. 3-6. The highest location from the binary flame map defined the flame height for each snapshot in time. A time series of flame height is shown in Fig. 3-7. The rapid growth of the fire up the flue space is captured during the first minute of the test, after which the flame stabilized at the fifth and sixth tier, 1.7-2 m (5.5-6.5 ft). The reduction in flame height starting at 350 s also coincides with the drop in HRR shown in Fig. 3-3.

The smoke layer height was determined using the converted luminosity image, Y (see Fig. 3-8). A single profile from each image was extracted along the vertical structure used to support the ML-ASRS containers. This vertical support structure spanned from the floor of the enclosure to a height of 2.6 m (8.5 ft). This location provided a dark background for which any smoke would locally increase the image intensity with minimal interference from flames. Smoke measurements above this vertical support structure were not possible due to the increased background intensity. A sample intensity profile, shown in Fig. 3-9, shows increased intensity from smoke on the left (the top of the ML-ASRS support structure) and a drop in intensity on the right (the bottom of the enclosure). An intensity threshold of 15 counts, was selected to define the smoke layer height. This threshold value was close to the intensity of the smoke layer itself, as to reduce the influence of image noise in other parts of the frames on

smoke layer height detection. The smoke layer height, as defined here, is an estimate since the gradient from high intensity to low intensity spans a distance of approximately 0.3 m (1 ft).

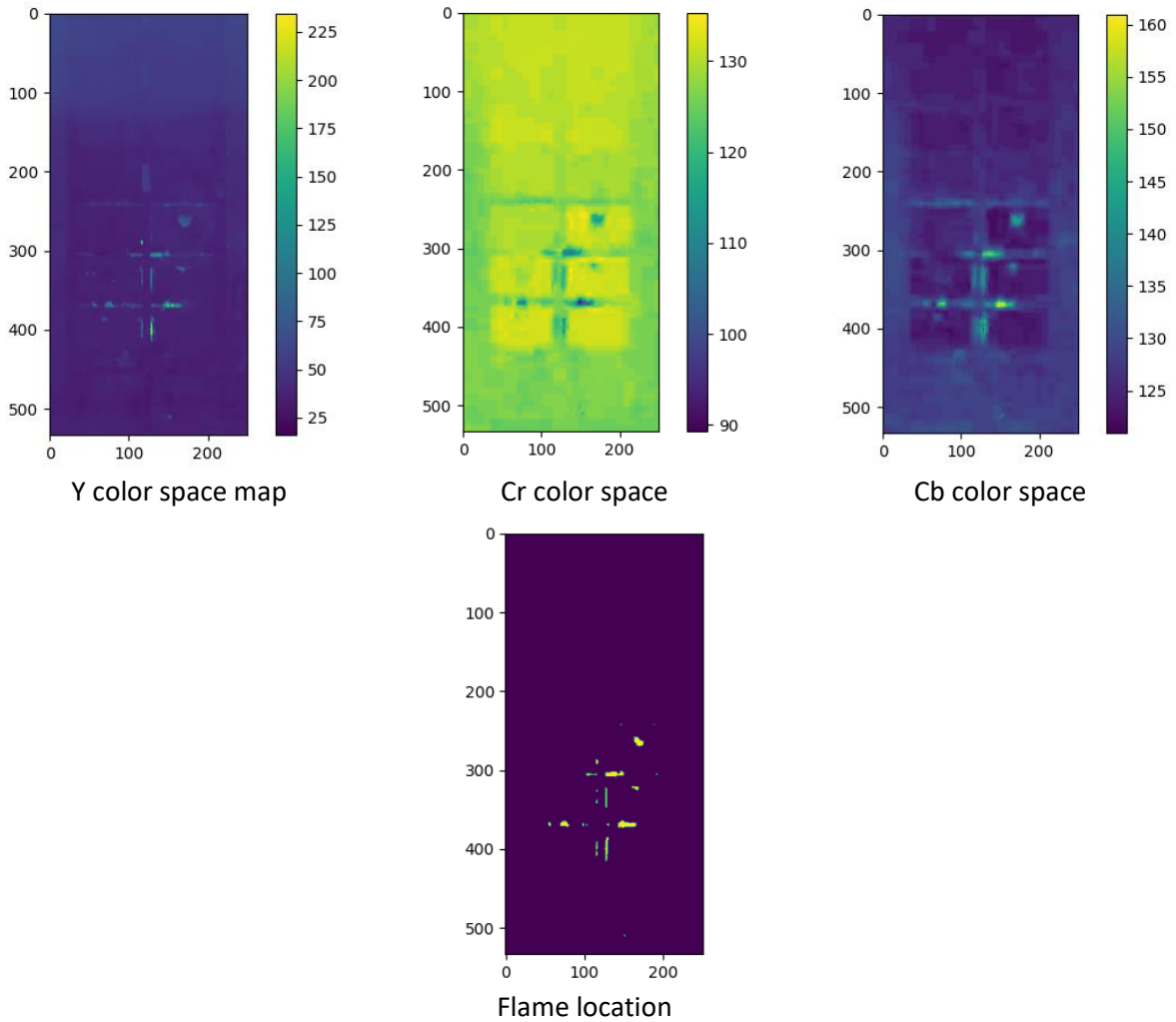


Figure 3-6: Sample images of color space transformation and resultant flame location as determined using Eqs. 3-1 and 3-2.

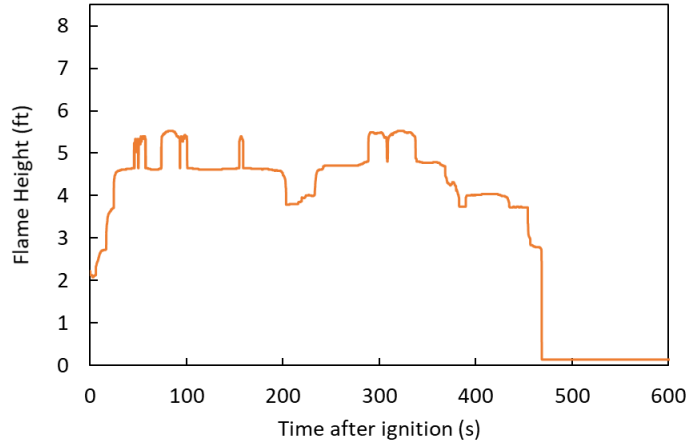


Figure 3-7: Flame height over time extracted from video for solid-walled ML-ASRS at 15% O₂.

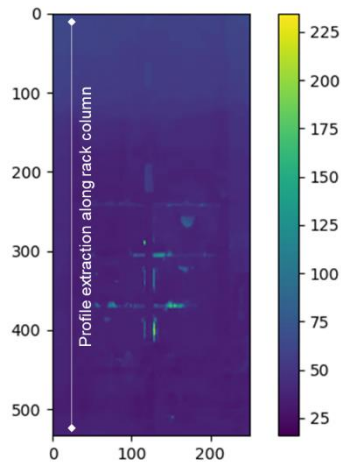


Figure 3-8: Image highlighting the smoke profile extraction location along the vertical support riser.

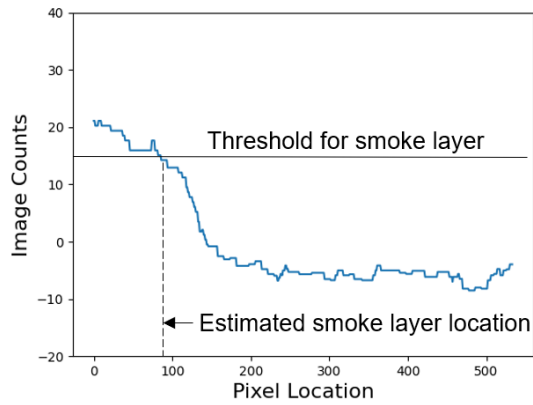


Figure 3-9: Sample profile used to estimate the smoke layer height.

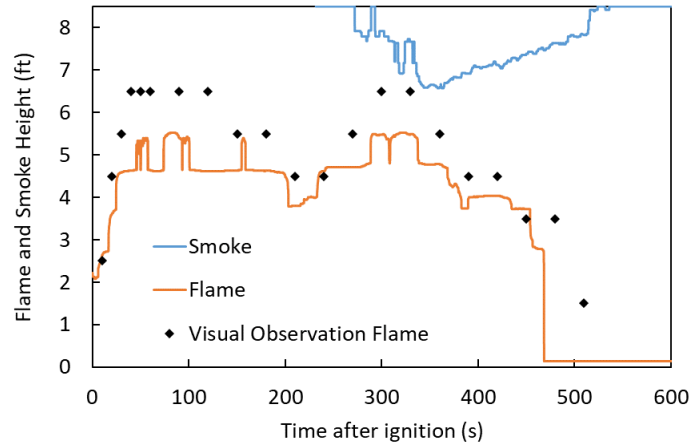


Figure 3-10: Smoke layer and flame height over time extracted from video for solid-walled ML-ASRS at 15% O_2 . The black symbols represent flame height extraction based on visual observation of the videos.

The extracted flame and smoke layer heights are plotted together for comparison in Fig. 3-10, with smoke layer height estimation only possible to a height of 2.6 m (8.5 ft). The effect of the smoke on the fire growth is evident as the minimum height occurs at the time when the fire size begins to decrease. The profiles for the smoke and flame height do not intersect as expected, with the gap attributed to limitations in estimating each profile from the RGB images. As stated earlier, uncertainty for the smoke layer can be about 0.3 m (1 ft) as a threshold value was taken at the upper part of the intensity profile in Fig. 3-9 to minimize noise during extraction. Additionally, the flame height also has some uncertainty due to low signal levels relative to the background. Visual extraction of the flame height, as seen by the points in Fig. 3-10 show areas where the extraction algorithm limitations prevent detection of lower intensity flames. For example, the flame at time = 300 s in Fig 3-2 is along the inner wall of the container within the flue at a height of 2 m (6.5 ft), however, the flame extraction was unable to capture this low luminous flame. In a warehouse with significantly more volume, the development of this smoke layer is not expected. The local drop in oxygen concentration within the test enclosure was estimated to determine the conditions which limited fire propagation.

The oxygen concentration measurement for testing was provided by extractive gas sampling at three different locations in the enclosure. The three gas samples were combined and supplied to a single gas analyzer for oxygen concentration measurements. The local concentration at the top sampling location can be determined by making two assumptions: the extraction rates at each port are identical and the two lower locations have the same reading. The local drop in oxygen concentration at the top sampling location caused by the smoke can then be determined using Eq. 3-3,

$$O_{2,top}(t) = 3 \times O_2(t) - 2 \times \overline{O_2(t)}_0^{100} . \quad 3-3$$

In the equation, the gas concentration at the two lower extraction ports is estimated by averaging the measured concentration over the first 100 seconds of the test, where no smoke was present. The resultant local oxygen concentration, $O_{2,top}$, can be calculated and is shown in Figure 3-11 along with the

original measurement. Locally, the oxygen concentration reached 14.5% on average and resulted in a successful test. The LOC_{FP} for the empty solid-walled containers should therefore be 14.5%.

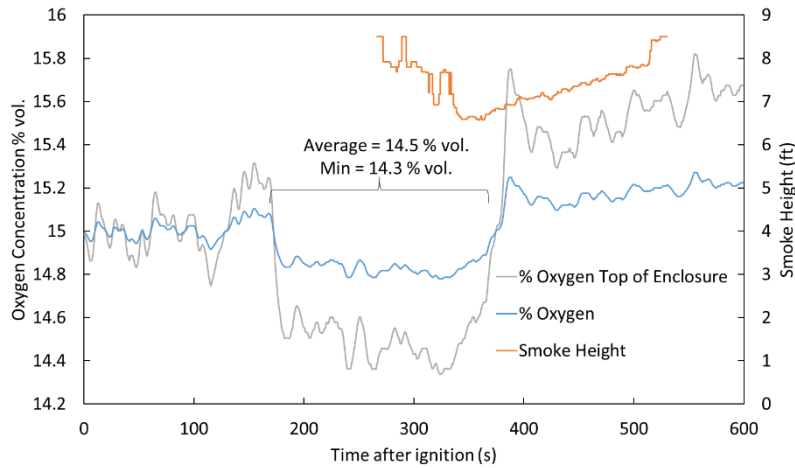


Figure 3-11: Overlay of smoke layer height (orange), measured oxygen concentration (blue) and the estimated oxygen at the top of the enclosure due to smoke (grey).

The vented containers were tested next, over a range of 15-17% oxygen. Figure 3-12 shows snapshots of the fire development for these containers at a concentration of 17%. Initially, the fire grew similarly to the solid-walled container tests. The fire was primarily within the flue space for the first 45 s. Once the sides of the containers were compromised, the fire spread and grew within the containers themselves. The oxygen concentration was not low enough to prevent continued fire propagation with flames escaping the top of storage array at 270 s. At this point, the igniter was turned off and the fire continued to grow until manual suppression was applied after 300 s.

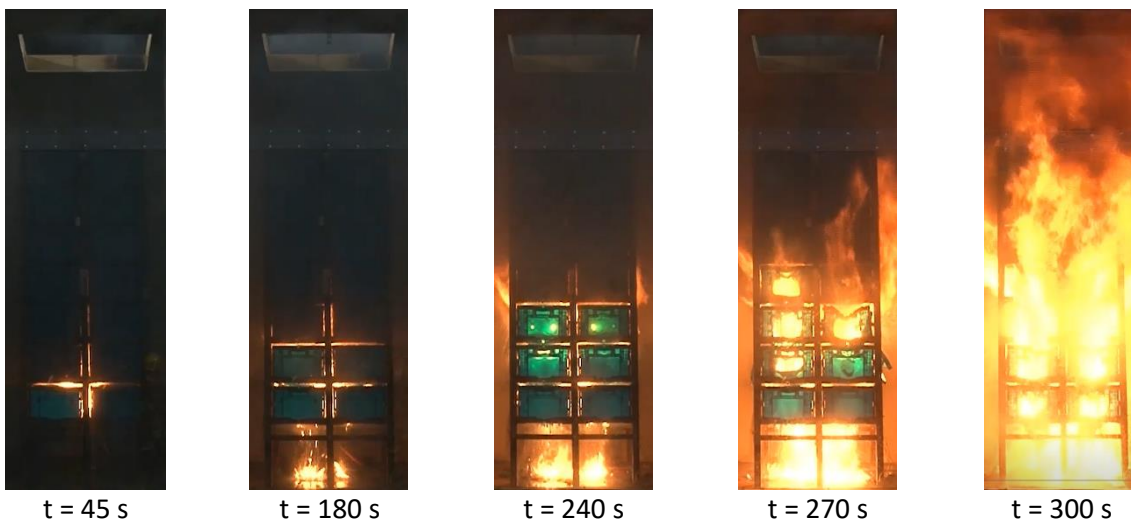


Figure 3-12: Images of fire development for vented ML-ASRS at 17% O_2 at selected times after ignition.

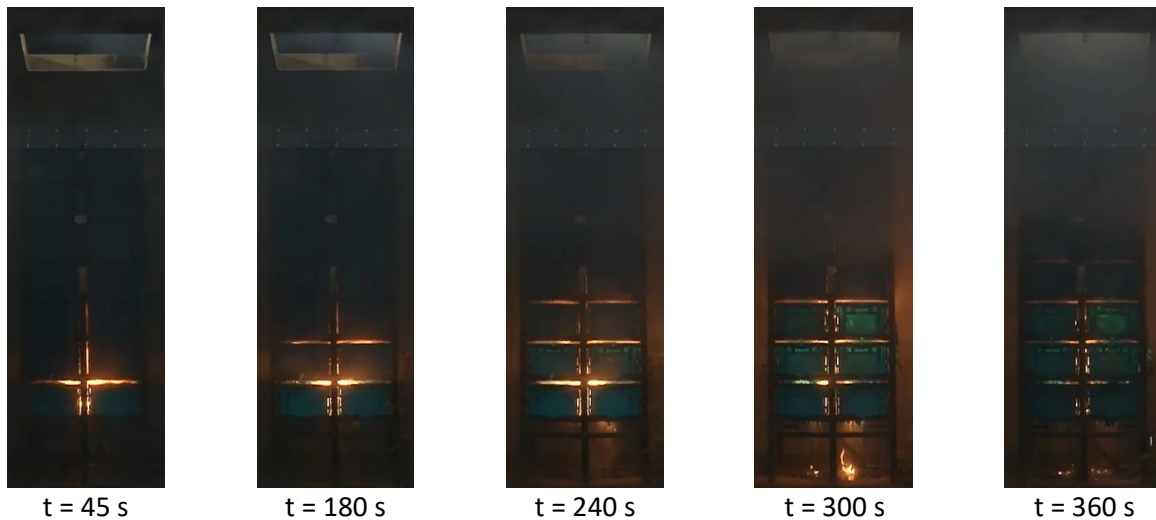


Figure 3-13: Images of fire development for vented ML-ASRS at 16% O₂ at selected times after ignition.

The fire propagation was better controlled at lower oxygen concentrations. A reduction to 16% oxygen resulted in a more controlled flame (see Fig. 3-13). The fire slowly grew to the fourth tier over a period of 300 s. Flames were more visible for the vented container tests as the thin side walls provided a more translucent structure for visualization. A smoke layer, similar to that observed during the solid-walled test at 15%, developed within the enclosure around 300 s. In the presence of the smoke layer, fire propagation stopped, and flames dropped down to the first tier of storage around the igniter. The snapshots from the test also show burning of melted plastic at floor level, highlighting the ability of the container material to sustain burning at this oxygen concentration. Vented container testing at 15% oxygen showed no burning at the floor with limited fire propagation up the storage array.

The HRR data for the vented container tests are shown in Fig. 3-14, with trends similar to those of the solid-walled container tests. At 17% oxygen, as was evident from the snapshots, the HRR shows uncontrolled fire growth until manual extinguishment at 300 s. The HRR at 16% oxygen, represented by the orange line, shows a slow growth to a point where the fire stabilizes for a period of 60 s. Thereafter, the HRR slowly drops and the fire settles to around the igniter location. The decrease in fire size and HRR was again affected by the presence of a smoke layer in the upper part of the test enclosure. Applying the identical approach used for the solid-walled test, the local oxygen concentration dropped to a minimum of 14.5% during the 16% oxygen test (see Fig. 3-15). The limited propagation and successful outcome of the test conducted with 16% oxygen inlet flow was therefore the result of the local oxygen reducing to 14.5% as a result of the smoke.

Notably, fire was observed along the outer faces of the array during the tests. Based on this observation, evaluation of horizontal flame spread was conducted by including an additional column of containers within the test enclosure. The HRR curve, labeled 16% added column, shows that no further growth resulted with the additional containers (see Fig. 3-14). The HRR curve was similar to that of the 15% oxygen case with little growth occurring past the third tier of commodity. The reduced HRR may be due to test uncertainty as little smoke buildup occurred during the test. A post-test damage assessment

of the containers showed that flame propagation was primarily in the vertical direction up the test array with minimal damage present in the additional column.

The fire propagation during the test with 15% O₂ was not affected by smoke. There was no burning of plastic at the floor level and propagation was limited to below the third tier of storage. Therefore, the LOC_{FP} for the vented walled containers is slightly higher than that of the solid-walled containers, 15% vs. 14.5% oxygen.

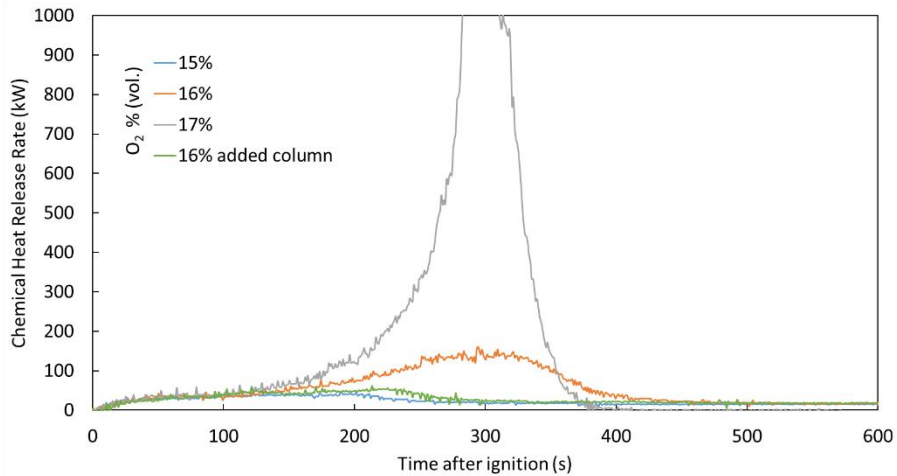


Figure 3-14: Chemical HRR for vented ML-ASRS containers in the range 15-17% oxygen.

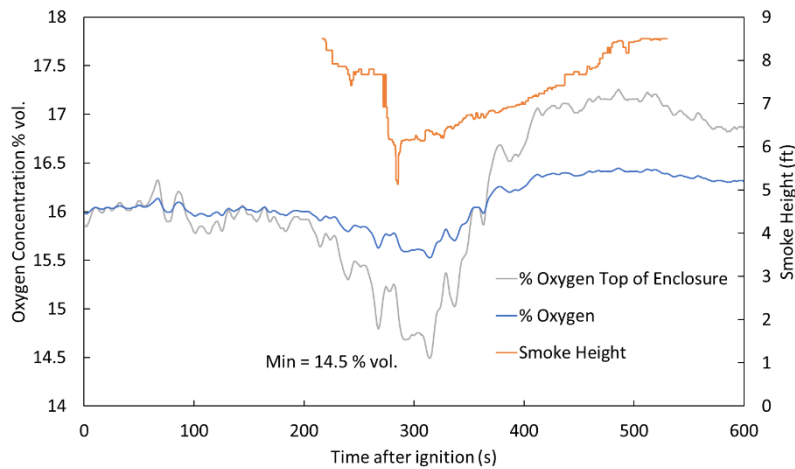


Figure 3-15: Overlay of smoke layer height (orange), measured oxygen concentration (blue) and the estimated oxygen concentration at the top of the enclosure due to smoke (grey). Oxygen was set to 16%.

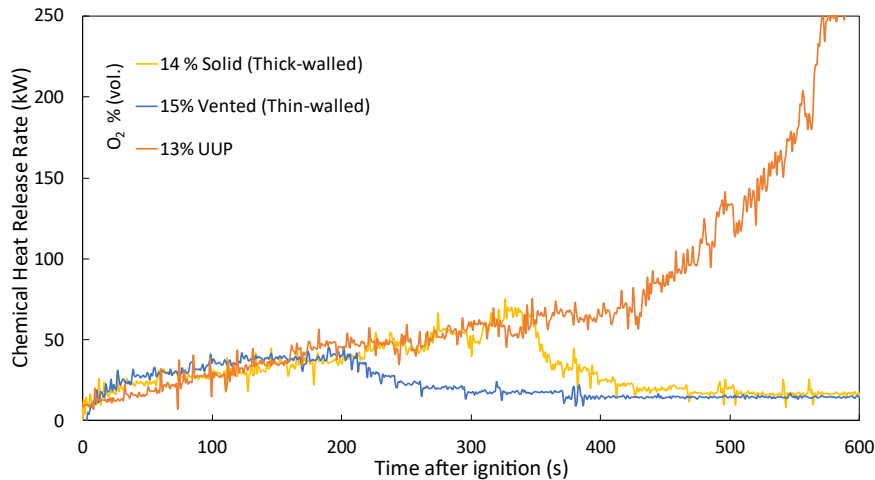


Figure 3-16: Chemical HRR of the two ML-ASRS containers relative to UPP near their respective LOC_{FP} .

The difference in LOC_{FP} between the vented (thin-walled) and solid (thick-walled) containers was driven by the amount of participating material available for combustion. The vented containers have lower mass and thinner side walls compared to the solid-walled containers. The effect of participating material on the fire growth is highlighted in Fig. 3-16. Here, HRR curves compare the fire growth between the two containers near the LOC_{FP} . The fire growth from standard uncartoned unexpanded plastic (UUP) at LOC_{FP} is also shown on this figure. The initial fire growth rates in all three tests are similar, with differences occurring at the point where the material around the igniter area is depleted. The thin-walled vented container test, having the least amount of material for combustion, decays first. The thick, solid-walled container test shows a decay in HRR about 100 s later, as the thicker solid sidewalls provided more mass for combustion. Ultimately, the HRR for the UUP test, at 13% oxygen shows continued fire growth. The ML-ASRS containers represent about 20-30% of the mass present in the UUP testing. Additional plastic commodity within the ASRS containers would likely lower the LOC_{FP} to match that of the UUP commodity (13% oxygen). Containers which are empty or filled with a small amount of noncombustible material can be protected at conditions of 14.5% oxygen.

3.1.2 Impact of Internal Contents

The effect of stored goods within the ML-ASRS containers was tested by placing corrugated boxes, described earlier, in each container. A series of tests using 11-14% oxygen was conducted to evaluate differences in fire propagation. Tests at 12% and 14% oxygen resulted in protection failure, while three tests at 11% oxygen met the success criteria for LOC_{FP} . Figure 3-17 provides images of a test that was conducted at an oxygen level of 12%. Generally, flames were not as visible as with the empty container tests. At this oxygen concentration, there was no visible burning of the plastics; however, as the plastics melted, exposing the internal contents of each container, the corrugated boxes began burning. Flames were visible on the outer faces of the storage array after 400 s. The fire from the boxes continued melting additional containers causing uncontrolled fire growth. Ultimately, flames were observed at the exit of the enclosure prior to the 10-minute test termination point. The HRR curve for the 12% oxygen test in Fig. 3-18 shows a rapid increase in HRR at the 550 s mark. Although a smoke layer occurred

within the enclosure, any reduction in oxygen level at the top failed to prevent continued fire growth within the storage array.



Figure 3-17: Images of fire development for vented ML-ASRS with corrugated contents at 12% O₂ at selected times after ignition.

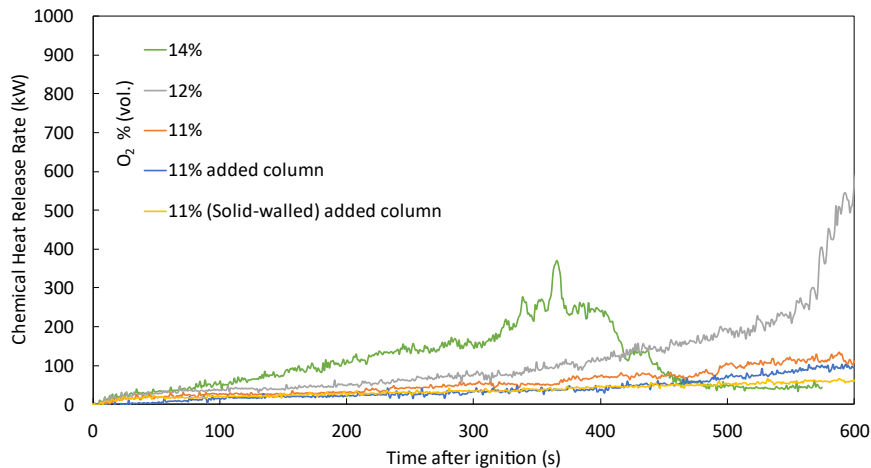


Figure 3-18: HRR curves for ML-ASRS containers with internal corrugated cardboard contents at oxygen concentrations between 11 and 14%.

Three different tests at an oxygen concentration of 11% demonstrated successful protection with no uncontrolled fire growth and no flames present along the top of the array. HRR curves for the three tests are shown in Fig. 3-18. The addition of a third column of containers did not affect the fire growth. Differences in the plastic containers (vented vs. solid-walled) made no difference in the successful outcome of the tests as the internal boxes played the dominant role in fire growth. Figure 3-19 (a) and (b) highlight the damage caused during the 11% and 14% oxygen tests, respectively. At 11% oxygen, melting of the containers was present up to the second tier of the fuel array, whereas for 14% oxygen

the containers melted away exposing a significant portion of the corrugated products within, promoting additional fire growth.

a)



b)



Figure 3-19: Post-test damage at 11% oxygen (a) and 14% oxygen (b) for the vented ML-ASRS with corrugated boxes within the containers.

The presence of corrugated boxes, which have a lower LOC_{FP} than the plastic containers, results in a lower LOC_{FP} when compared to the empty ML-ASRS arrangement. An LOC_{FP} of 11% for the filled containers brings the value in line with the 11% LOC_{FP} previously defined for cartoned commodities [3].

3.1.3 Impact of Flue Space

An increase in flue space was evaluated to determine how the flame propagation can change with increased separation distance between containers. The additional space within the flue, 15 cm (6 in.) vs. the previously tested 5 cm (2 in.), can result in lower radiation heat fluxes to adjacent containers across the flue, leading to decreased flame spread. Figures 3-20 and 3-21 show the flame progression for two tests of vented containers at 18% and 19% oxygen, respectively. At 19% oxygen, uncontrolled fire propagation occurred, resulting in a failed test. Significant burning of melted plastic occurred at floor level. This burning pool of plastic provided additional heating of the containers above, contributing to the strong fire growth up the storage array.

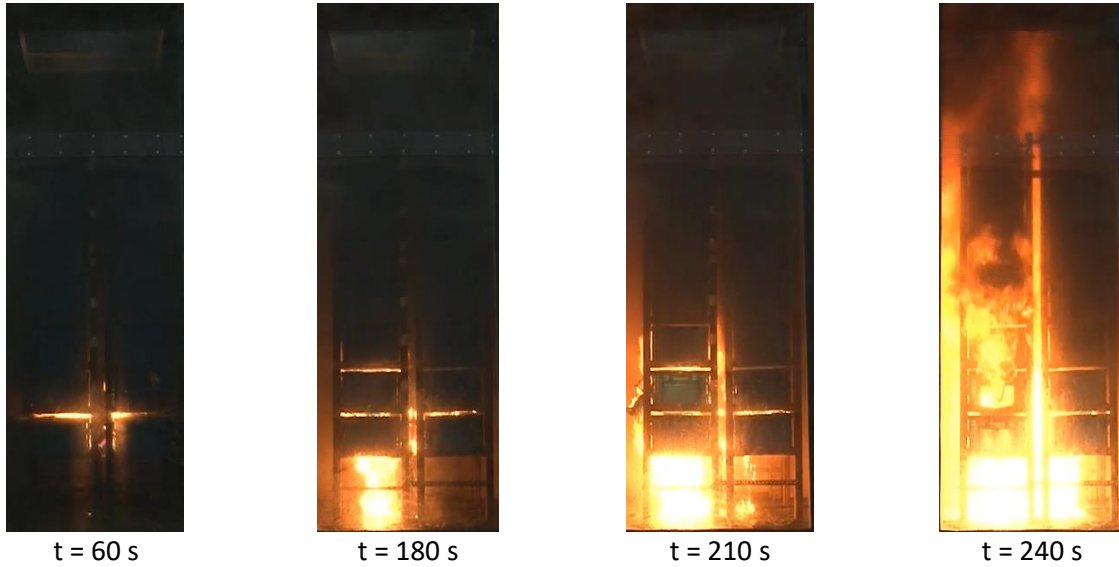


Figure 3-20: Images of fire development for vented ML-ASRS with 15-cm (6-in.) flue space at 19% oxygen at selected times after ignition.

The test at 18% oxygen resulted in a significantly smaller amount of burning at floor level (see Fig. 3-21). The fire at the floor was not large enough to contribute to the fire growth. Fire propagation stopped at the second tier and was limited by the amount of material available in the area surrounding the igniter. Minimal material remained around the igniter, with the thin walls of the vented containers melting away (Fig. 3-22a) and pooling at the floor (Fig. 3-22b).

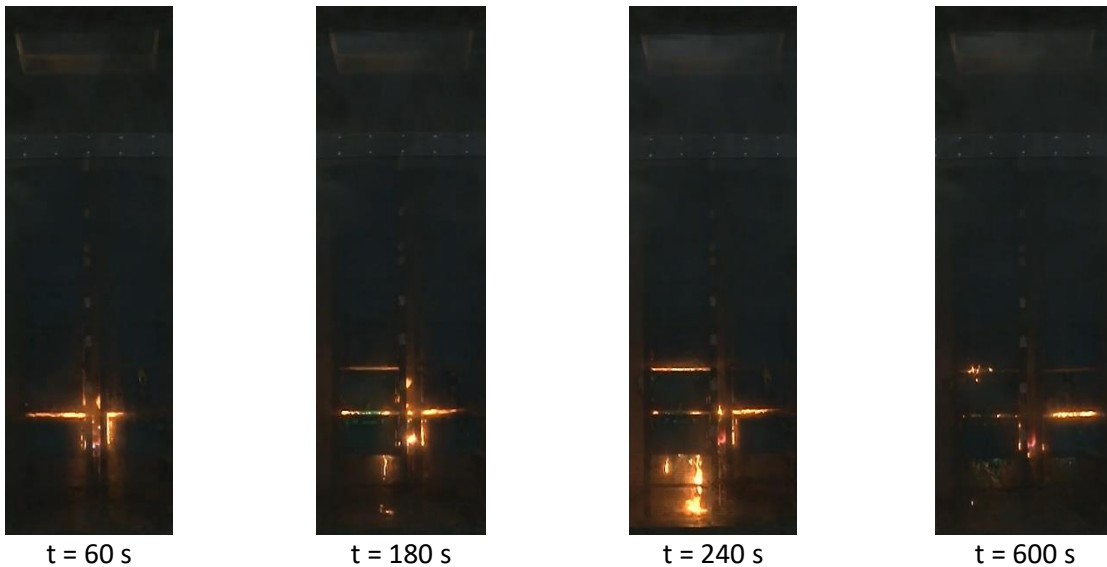


Figure 3-21: Images of fire development for vented ML-ASRS with 15-cm (6-in.) flue space at 18% oxygen at selected times after ignition.

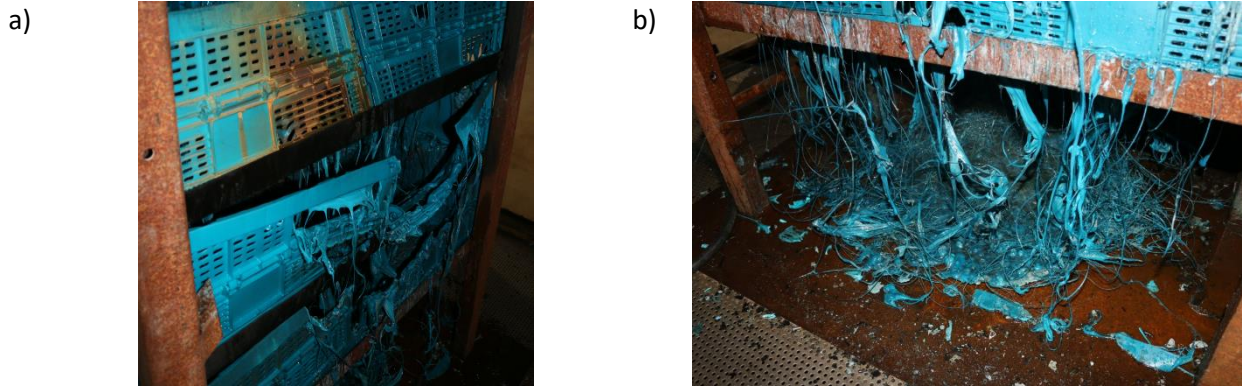


Figure 3-22: Post-test damage showing sidewall melting (a) and pooling at the floor (b), following the vented container test with 15-cm (6-in.) flues and 18% oxygen.

Tests conducted with the heavier solid-walled containers showed fire propagation characteristics similar to that of the thin, vented containers, although at oxygen levels 1% lower. HRR curves for both the vented and solid-walled containers are shown in Fig. 3-23, and show uncontrolled fire growth at oxygen levels of 18% and 19%, respectively. The thicker sidewalls of the solid-walled containers contributed more material to the fire, resulting in the 1% decrease in LOC_{FP} .

The larger flue space resulted in significantly higher LOC_{FP} . These changes were caused by a reduction in the mass of material near the ignition source. Fire growth occurred within the containers themselves, and not primarily within the flue space. It is expected that a different ignition location or an ignition source wide enough to span a larger part of the containers would reduce the LOC_{FP} closer to that measured in the 5-cm (2-in.) flue space test. In the case of the previously tested UUP commodity, at a 15-cm (6-in.) flue space, a significantly lower LOC_{FP} of 13%, was required due to the presence of more material for combustion [3]. In those previous tests, fire growth also occurred within the plastic pallets and was not limited to the flue space.

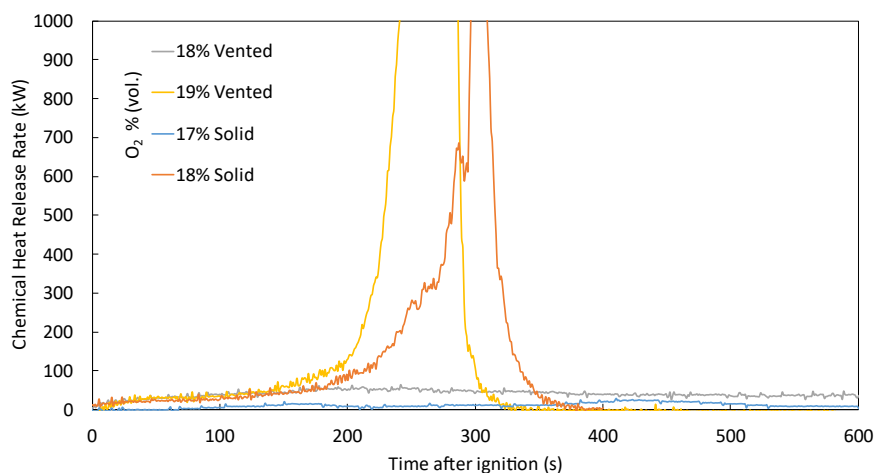


Figure 3-23: HRR curves for ML-ASRS containers at a 15-cm (6-in.) flue space at various oxygen concentrations.

The wider flue space had a similar effect on containers with corrugated contents. A 1% increase in oxygen concentration, 12% instead of 11%, provided suitable conditions for limited fire propagation and no uncontrolled fire growth. The HRR curves in Fig. 3-24 show uncontrolled fire growth at 13% oxygen with very little growth at 12%. At 13%, the fire grew rapidly once the plastic container walls melted. The corrugated products within burned away exposing additional corrugated contents as the plastics melted away (see Fig. 3-25). The separation between the internal contents and the igniter results in a reduction in corrugated material affected by the igniter. This proximity ultimately contributed to the higher LOC_{FP} . It is expected that an ignition scenario originating within the containers themselves would likely eliminate that flue space effect, resulting in an LOC_{FP} of 11%, matching that found in the 5-cm (2-in.) flue space test.

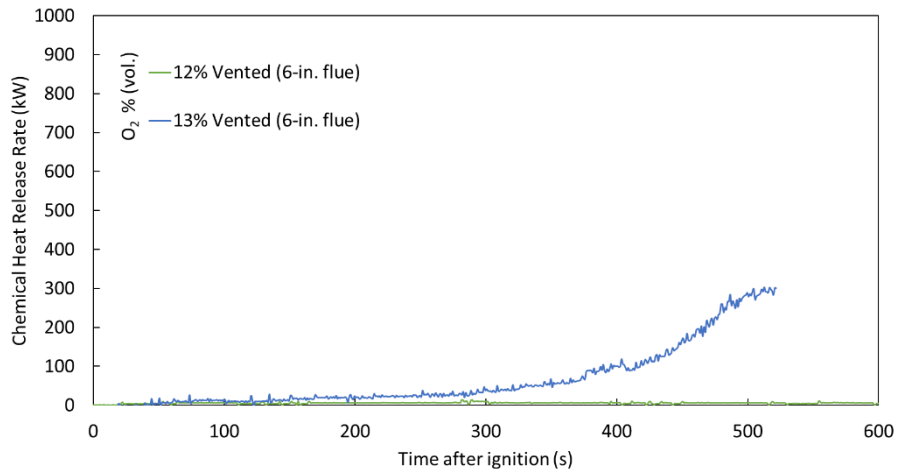


Figure 3-24: HRR curves for vented ML-ASRS containers at different oxygen concentrations with internal corrugated cardboard contents and a 15-cm (6-in.) flue space.



Figure 3-25: Post-test image of damage to the vented ML-ASRS containers and the internal corrugated boxes.

3.2 Frozen Food Testing

3.2.1 Impact of Frozen Food Commodity

Five tests were conducted to evaluate variations in LOC_{FP} caused by high-moisture-content, low-temperature items placed within corrugated boxes. Four of the tests, conducted over a range of 13-15% oxygen, used Class 3 corrugated boxes with frozen food contents. A final test using wax-saturated boxes yielded an additional data point for evaluating differences in the packaging material. Fire development in the frozen food commodity is shown in Fig. 3-26 at an oxygen concentration of 13%. Fire growth was quite different from that of the ML-ASRS tests shown earlier, with propagation occurring primarily within the flue space. At 13% oxygen, the fire grew rapidly to the second tier of commodity 30 s after ignition. There was no lateral spread visible and the fire size dropped down to within the first tier of storage within the first minute of the test. Sustained ignition over the ten-minute test duration provided no increase in fire growth and the test showed successful ORS protection.

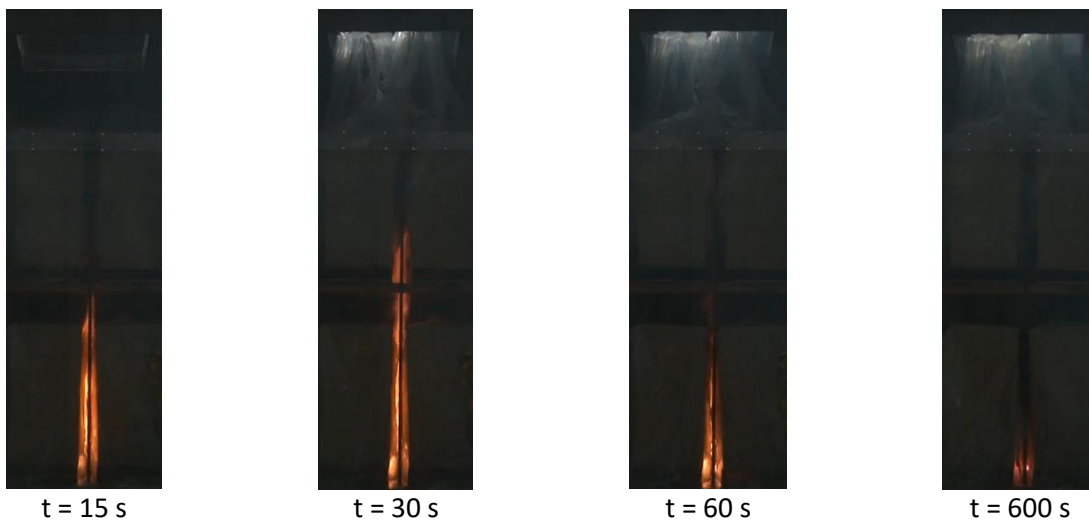


Figure 3-26: Images of fire development for frozen food in corrugated boxes at 13% oxygen at selected times after ignition.

Subsequent tests of frozen food commodities at higher oxygen concentrations resulted in failed protection outcomes. As shown in Fig. 3-27 at 14% oxygen, the fire continued to grow after reaching the second tier of commodity at 45 s. Burning of commodity in the second tier resulted in visible flames above the storage arrangement within 1 minute into the test, resulting in test failure. Over that time, additional tiers in a higher storage arrangement would have provided material for further growth. The igniter was shut off at 110 s and the fire size quickly dropped, with no flames present at 140 s.

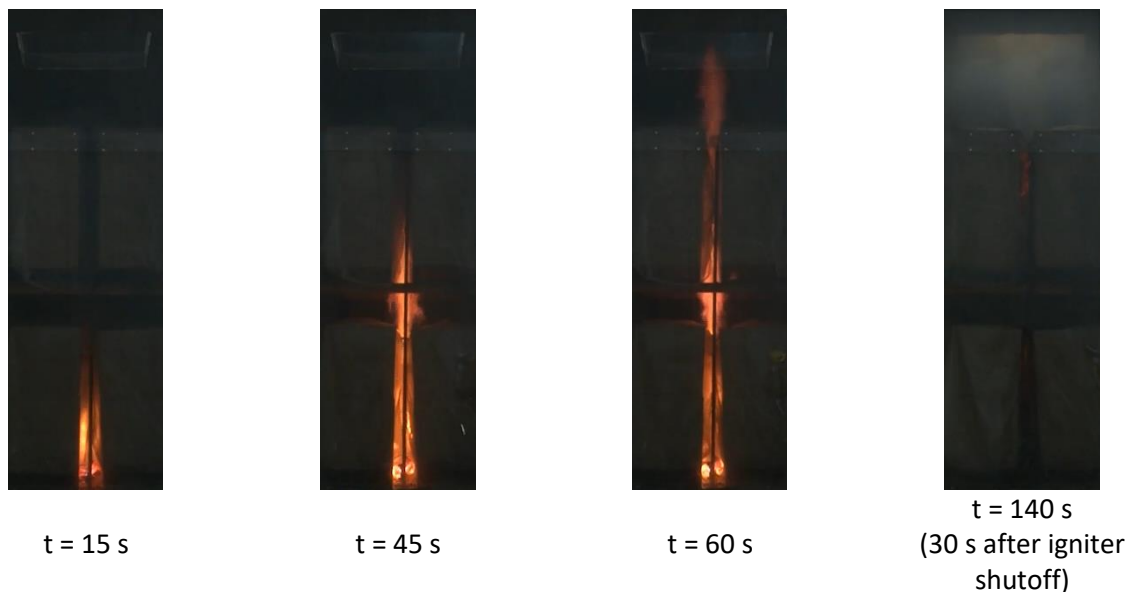


Figure 3-27: Images of fire development for frozen food in corrugated boxes at 14% oxygen at selected times after ignition.

Testing of the frozen food was repeated at 13% oxygen using both Class 3 and the wax-saturated packaging material. HRR curves for the frozen food tests are shown in Fig. 3-28. The two Class 3 tests at 13% oxygen yielded peak HRR values of approximately 100 kW. The first test, as shown in Fig. 3-26, was successful. In the second test, flames were present above the second tier, resulting in protection failure. Although the fire ultimately dropped in size with the sustained ignition source, the flames penetrating above the storage array could have ignited commodity above had it been present during the test, potentially yielding further flame propagation.

The rapid fire growth observed during the frozen food testing was driven by the external packaging materials. The material is thin, and heats quickly. For the case of the wax-saturated boxes, the hydrocarbon wax contributed to fast flame spread, upon 2nd tier ignition as seen in the second increase in the HRR curve. This yielded a peak HRR value of approximately 200 kW (see Fig. 3-28), and where flames reached above the second tier resulting in protection failure. Damage from the frozen food testing, as shown in Fig. 3-29, shows charring of the external packing along the inner face of the second tier for the tests at 13% oxygen. The first test at 13% oxygen showed little damage within the second tier, while the second Class 3 and wax-saturated box tests showed more damage to the packaging. The frozen food was relatively undamaged in all tests. Figure 3-30 provides a picture of a frozen food meal removed from the first tier near the igniter. The majority of the food was still frozen with only slight burning of the plastic tray. The thermal sink created by the frozen food relative to standard Class 3 commodity is the main driver for the difference in LOC_{FP} , with a successful test at 13% instead of 11.1% oxygen for the standard commodity [3].

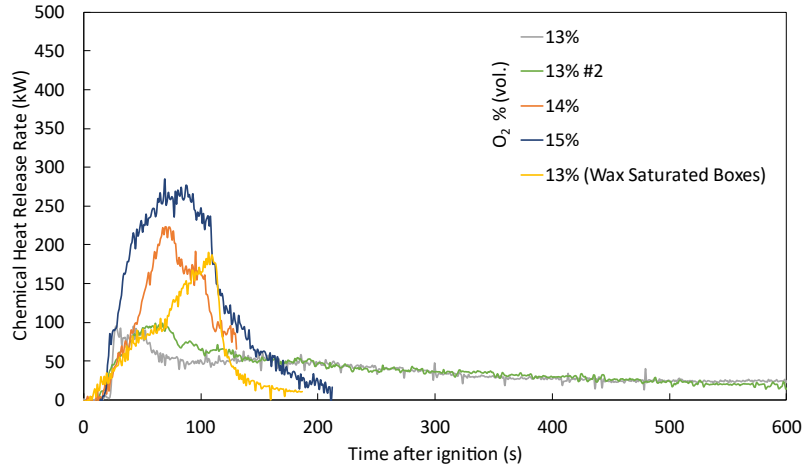


Figure 3-28: HRR curves for the frozen food fire testing using standard and wax-saturated corrugated packaging.

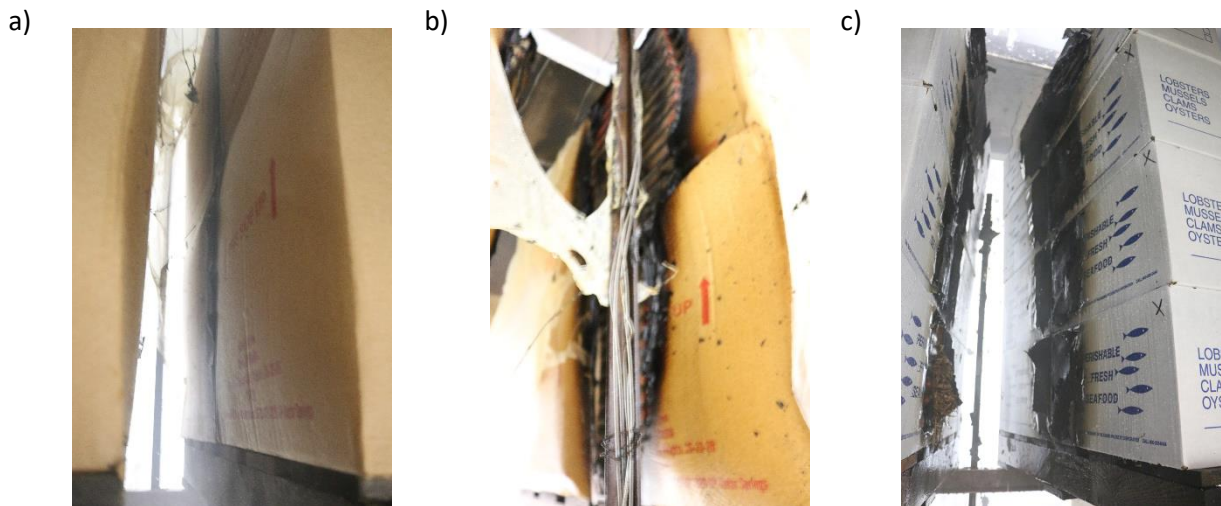


Figure 3-29: Post-test damage at the face of the second tier for frozen food stored in standard corrugated packaging, tests 1 (a) and 2 (b), and wax-saturated packaging (c) at 13% oxygen.

The low oxygen concentrations required for protection of the frozen food commodities can be partially attributed to local oxygen increases caused by the release of air from within the boxes as the fire burns through the side walls of the packaging. Removal of the air within the boxes is unrealistic as the packaging is typically sealed and protected from the outside environment. Increases in the measured oxygen concentrations during the frozen food tests are shown in Fig. 3-31. The 1% increases in oxygen were likely caused by release of trapped air from within the corrugated boxes to the enclosure. The void volume within the boxes, neglecting the thickness of the paper cups, represents about 8% of the total volume within the enclosure. Although a 1% increase was measured within the enclosure, the local concentration near the fire is likely higher (i.e., the location where air escapes through the generated openings in the boxes) promoting flame propagation as more boxes are breached by the fire.



Figure 3-30: Damage to frozen food meal within first tier after the test at 13% oxygen.

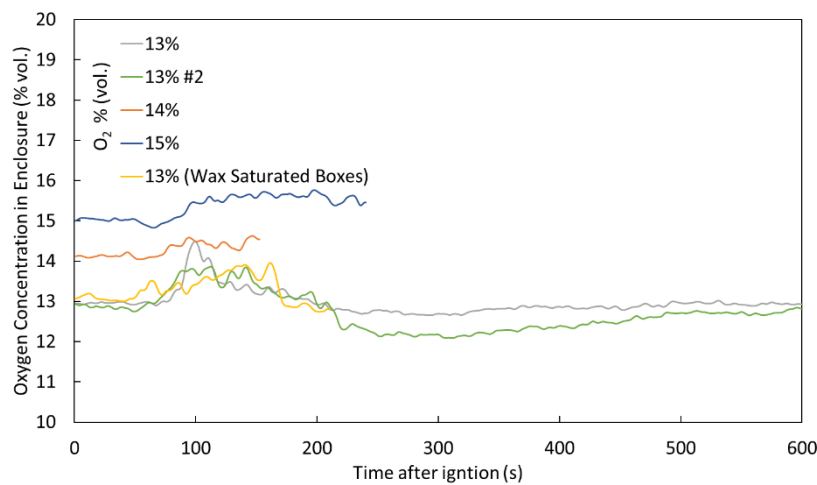


Figure 3-31: Measured oxygen concentration for each frozen food test. Increases were caused by the escape of atmospheric air within each box during the fire test.

Establishing an appropriate LOC_{FP} for frozen food packaging required the use of statistical information from previous tests of corrugated commodities. Two of the three tests conducted at 13% oxygen resulted in protection failure. The failure rate equates to a fire propagation probability of 67%. Statistical analysis for the previously tested corrugated commodities used logistic regression to determine the fire propagation probability based on the test failures (see Fig. 3-32) [3]. The LOC_{FP} for corrugated commodities was defined at the oxygen concentration resulting in a 5% probability for fire propagation. The previously determined regression curve shape represents the failure probability for corrugated commodities and is assumed to be representative of the behavior of the external packaging material used in the frozen food tests. Application of the regression curve from a failure rate of 67% to 5% fire propagation probability yields a 0.5% difference in oxygen concentration. The resultant 0.5% difference in oxygen concentration brings the recommended LOC_{FP} for frozen foods from 13% to 12.5%, targeting a 5% fire propagation probability. The 1.5% increase over standard corrugated commodities shows a benefit of the frozen food; however, the fire growth through the packaging material was still dominant, which prevented any substantial changes in LOC_{FP} .

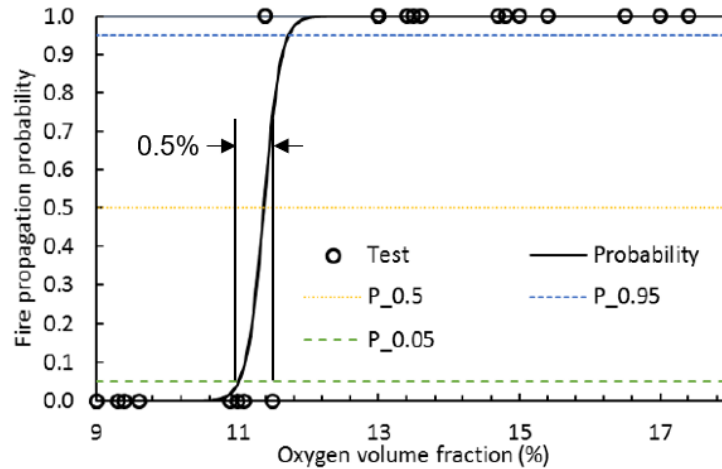


Figure 3-32: Fire propagation probability by oxygen concentration estimated for cartoned commodities [3]. Brackets highlight the 0.5% delta between 67% and 5% fire propagation probability.

3.2.2 Impact of Moisture Content

The targeted moisture content of the external corrugated boxes was between 7-13%. Moisture content was measured from samples taken prior to ignition and are presented in Table 3-2, arranged based on the test order. The external moisture increased with each subsequent test. The increase, of approximately 1% for each test, was attributed to opening of the freezer to extract the test commodity between adjacent tests. It was expected that increased moisture content would provide more favorable conditions for protection. However, the repeat test at 13% oxygen demonstrated no protection benefit from the increased moisture. Protection failed in the repeat test although the moisture content was 4% higher. It is possible that larger changes in moisture content may provide benefits to the LOC_{FP} . But for the range of conditions representative of freezer conditions, the increased moisture did not provide measurable improvement.

Table 3-2: Measured moisture content of the corrugated cardboard packaging and the test results for each frozen food fire test.

Packaging Material	O ₂ % (vol.)	Moisture Content (%)	Test Result
Corrugated Box	13	12	Pass
Corrugated Box	15	14	Failure
Corrugated Box	14	15	Failure
Corrugated Box	13	16	Failure
Wax Box	13	N/A	Failure

4. Summary and Recommendations

Large-scale fire testing of ASRS and frozen food storage was conducted to determine the LOC_{FP} for ORS protection. The differences in storage geometry for the ASRS and lower temperatures in frozen food applications were evaluated to understand changes to the LOC_{FP} as a result of those altered conditions. A test enclosure was used to provide a well-controlled environment of 11% to 18% oxygen over the range of tests. Fire propagation was observed for each test configuration to establish the LOC_{FP} as summarized in Table 4.1. Conditions for non-combustible contents are representative of scenarios where the containers are either empty or with a small quantity of non-combustibles stored.

Table 4-1: LOC_{FP} for ASRS and frozen food commodities tested in this work. Standard cartoned and uncartoned commodity values have been added for comparison.

Storage Conditions	LOC_{FP} (% vol.)
Uncartoned Commodity	13
Cartoned Commodity	11
ML-ASRS (PP with Non-Combustible Contents)	14.5
ML-ASRS (PP with Uncartoned Plastic Contents)	13
ML-ASRS (PP with Cartoned Contents)	11
Frozen Food Storage	12.5

The experimental results showed that

- For ML-ASRS:
 - The mass of the containers (thin vented vs. thick solid-walled) contributed to differences in the LOC_{FP} ultimately yielding an LOC_{FP} of 14.5% oxygen when empty or with non-combustible contents.
 - The contents of the containers are important. Internal corrugated boxes resulted in LOC_{FP} values consistent with standard corrugated commodities at 11% oxygen, while plastic contents bring the LOC_{FP} to 13%.
 - Wider flue space resulted in increased LOC_{FP} driven by decreased participation of combustible materials around the ignition location. Fire growth was not limited to the flue space and possible ignition differences would likely increase material participation, resulting in LOC_{FP} values matching those for narrow flue space.

- For Frozen Food:
 - The frozen meals packaged in corrugated cardboard behaved similarly to standard corrugated commodities in a reduced oxygen environment. Fire growth was mainly driven by the external packaging material.
 - The inclusion of the frozen food provided a slight benefit for the LOC_{FP} with a value of 12.5% oxygen as opposed to 11% for standard corrugated commodities. The benefit was attributed to the thermal sink provided by the frozen food resulting in little fire damage to the frozen food and minimal lateral spread into the storage array.

The LOC_{FP} has been shown to depend on storage material, geometry, and test conditions. It is important to note that the recommendations in this report are based on the conditions tested. Although engineering judgment can be used to further expand on the current recommendations, factors such as ignition scenario or stored material characteristics may result in changes to the LOC_{FP} that would require additional testing. Efforts to improve the ability of small-scale testing to match results from large-scale experiments are certainly important and will help improve future research efforts involving different commodities. Such efforts, however, are challenging as many effects such as storage geometry, fuel packaging and contents, and ignition source size and duration must be captured to adequately determine the LOC_{FP} .

References

1. Occupational Safety and Health Administration (OSHA), Regulation 29 CFR 1915.12 (a).
2. Yibing Xin and Mohammed M. Khan, "Flammability of combustible materials in reduced oxygen environment," *Fire Safety Journal*, vol. 48, no. 8, pp. 536-547, 2007.
3. Xiangyang Zhou, Yibing Xin, and Sergey Dorofeev, "Large-scale fire tests of oxygen reduction system (ORS)," in *The 3rd European Symposium on Fire Safety Sciences*, Nancy France, 2018.
4. Martin Nilsson and Patrick van Hees, "Advantages and challenges with using hypoxic air venting as fire protection," *Fire and Materials*, no. 38, pp. 559-575, 2014.
5. VdS 3527en, Inerting and Oxygen Reduction Systems, Planning and Installation, 2007.
6. prEN 16750:2014, Fixed Firefighting Systems - Oxygen Reduction Systems - Design, Installation, Planning and Maintenance, 2014, Draft.
7. ISO 20338:2019, Oxygen reduction systems for fire prevention: Design, Installation, Planning and Maintenance, 2019.
8. FM, Property Loss Prevention Data Sheets 4-13, Oxygen Reduction Systems, October 2021.
9. FM, Property Loss Prevention Data Sheets 8-34, Protection for automatic storage and retrieval systems, Oct 2020.
10. FM, Property Loss Prevention Data Sheets 8-29, Refrigerated Storage, May 2007.
11. Joseph F Hanlon, Robert J Kelsey, and Hallie Forcinio, *Handbook of Package Engineering Third Edition.*: CRC Press, 1998.
12. "The Databank - Top Frozen," *Frozen and Refrigerated Buyer*, pp. 8-9, May 2019.
13. "The Databank - Top Frozen," *Frozen and Refrigerated Buyer*, pp. 8-9, September 2019.
14. ISO 5167, Measurement of fluid flow by means of pressure differential devices inserted in circular cross-section conduits running full — Part 2: Orifice plates, 2003.
15. AGF Burner. <http://www.agfburner.com/>.
16. Franz Richter, Freddy X. Jervis, Xinyan Huang, and Guillermo Rein, "Effect of oxygen on the burning rate of wood," *Combustion and Flame*, no. 234, pp. 1-10, 2021.

17. Turgay Çelik and Hasan Demirel, "Fire Detection in video sequences using a generic color model," *Fire Safety Journal*, no. 44, pp. 147-158, 2009.
18. Supriya Sameer Nalawade, "Fire detection system using RGB color model," *International Journal of Engineering Science and Computing*, pp. 17516-17518, May 2018.

